1965

Static shear tests on longitudinally stiffened plate girders, December 1965

D. J. Fielding

P. B. Cooper

LEHIGH UNIVERSITY INSTITUTE OF RESEARCH

LEHIGH UNIVERSITY
Centennial Anniversary 1965-66

Longitudinally Stiffened Plate Girders

STATIC SHEAR TESTS ON LONGITUDINALLY STIFFENED PLATE GIRDERS

by

David J. Fielding
Peter B. Cooper

Fritz Engineering Laboratory Report No. 304.7

Submitted to the Welding Research Council Subcommittee
on Lehigh University Welded Plate Girder Project

STATIC SHEAR TESTS ON

LONGITUDINALLY STIFFENED PLATE GIRDERS

by

David J. Fielding

Peter B. Cooper

Lehigh University

Fritz Engineering Laboratory Report No. 304.7

December 1965

TABLE OF CONTENTS

ABSTRACT

This report describes eight static shear tests on four longitudinally stiffened plate girders. The experimental variables were the panel aspect ratio, transverse stiffener size, and longitudinal stiffener location and size. The primary objectives of the tests were to determine the effect of longitudinal stiffeners on the static behavior of plate girder panels subjected to high shear and to determine the contribution of longitudinal stiffeners to the static shear strength of plate girders.

The test setup and test procedure are described and the results are analyzed and discussed. It is concluded that the longitudinal stiffeners were effective in controlling web deflections, forcing separate tension fields to develop in the subpanels formed by the longitudinal stiffeners, and thereby increasing the shear strength of the girders.

1. INTRODUCTION

Prior to 1961 the provisions for the design of steel plate girders in most specifications were based on the theoretical buckling strength of the web. Theoretical and experimental research on transversely stiffened plate girders at Lehigh University has shown that there is no consistent relationship between the ultimate strength and the theoretical buckling strength of a steel girder.[1,2,3,4] Based on this work specifications for transversely stiffened plate girders for buildings are now being used in this country.[5]

In 1963 a new plate girder research project was started at Lehigh University with the general objective of determining the possible contribution of longitudinal stiffeners to the static load-carrying capacity of plate girders. One phase of this research has been to determine the static shear strength of longitudinally stiffened plate girders. Eight static shear tests were performed on four longitudinally stiffened plate girders during the spring of 1965. The purpose of this report is to describe the testing techniques, to present the test results and to offer the conclusions of the experimental investigation. The results of a parallel theoretical study have been presented separately in another report.[6]

2. TEST PROGRAM

2.1 Introduction

The primary objectives of the tests were to determine the effect of longitudinal stiffeners on the static behavior of plate girder panels subjected to high shear and to determine the contribution of longitudinal stiffeners to the static shear strength of plate girders.

The parameters which affect the shear strength of a longitudinally stiffened plate girder are the aspect ratio α (ratio of panel width to panel depth), web slenderness ratio β (ratio of web depth to web thickness), yield strain ϵ_y (ratio of yield stress to modulus of elasticity), longitudinal stiffener position η (distance from compression flange to stiffener divided by web depth), transverse stiffener size and longitudinal stiffener size. All of these parameters are further defined in the Nomenclature. By using the same web depth and nominal web thickness for all of the test specimens, the web slenderness ratio was kept constant. Since A36 steel was used for each specimen, the yield strain was kept near 0.0012. Thus, the principal variables for the test program were the aspect ratio, longitudinal stiffener position and the sizes of the transverse and longitudinal stiffeners. The actual values of the parameters for the eight tests are listed in Table 1.

2.2 Test Specimens

In Fig. 1 the sketches of test girders LS1 to LS4 show the plate sizes and stiffener locations. Overall girder length was 27 feet 6 inches. The basic design criterion was that the material properties and panel geometry should be the same or similar to those of the transversely stiffened plate girders previously tested in shear (Girders G6 and G7, Ref. 4) so that the test results could be compared. Practical ranges of the aspect ratio ($0.75 \leq \alpha \leq 1.5$) and longitudinal stiffener position ($0.2 \leq \eta \leq 0.5$) were used. Longitudinal, transverse, and bearing stiffeners were designed according to available theory.[5,7] Figure 2 shows a typical cross section with dimensions common to all girders. The longitudinal stiffeners and the transverse stiffeners were one-sided, but the bearing stiffeners, located at the end supports and at midspan, were symmetrical with respect to the plane of the web. To ensure that the girders would fail in shear, the flange plates were designed conservatively.

Coupons were cut from the ends of the ordered plates prior to fabrication as shown in Fig. 3. Actual plate dimensions measured at the locations indicated in Fig. 4 were obtained from the coupons. These measurements, averaged and tabulated in Table 2, were used in calculating cross-sectional properties.

Standard tensile tests were conducted to determine the mechanical properties of the component plates. On the coupons in Fig. 3 are sketched the locations of the tensile specimens. Two tensile specimens were taken from each web plate coupon (one perpendicular and one parallel

to the direction of rolling), and the average values of the measured properties from tests on these two specimens were used to represent the properties of the web plate material. Only specimens parallel to the direction of rolling could be obtained from the flange and longitudinal stiffener coupon plates. Static yield stresses (σ_y) obtained from the tensile tests are listed in Table 3, along with the percent elongation in eight inches and the chemical compositions obtained from the mill reports. For the web plates σ_y varied from 38.2 ksi to 48.6 ksi, while for the flange plates the variation was from 29.4 ksi to 30.5 ksi.

2.3 Reference Loads

Reference loads, calculated using the measured dimensions and yield stresses, were used to determine the loading increments and were later compared with the experimentally obtained ultimate loads. These reference loads include the theoretical web buckling loads (P_{cr}), the yield loads (P_y), and the theoretical ultimate loads for the same girders without longitudinal stiffeners (P_o). Since the load applied at midspan (P) was divided equally between the two supports (Fig. 5) the reference loads were equal to twice the calculated shear forces (V). The values of the reference loads are given in Table 4.

The theoretical web buckling load was calculated as follows:

$$\tau_{cr} = k^* \frac{\pi^2 E}{12(1-\nu^2)} \frac{1}{\beta^2} \quad (1)$$

$$V_{cr} = \tau_{cr} A_w \quad (2)$$

$$P_{cr} = 2 V_{cr} \quad (3)$$

Equation (1) is the same as that used in Ref. 2 except for k*, which here is the buckling coefficient for a longitudinally stiffened panel subjected to pure shear and having simply supported edges.[8] Equation (2) incorporates the area of the web A_w while equation (3) accounts for the loading condition.

The yield load P_y was computed according to beam theory using

$$V_y = \frac{\tau_y \, It}{Q} \tag{4}$$

where τ_y is the yield stress in shear, I is the moment of inertia of the cross section, Q is the static moment of the area above the neutral axis, and t is the thickness of the web. The yield stress in shear was calculated using tensile specimen results and Mises' yield condition, $\tau_y = \sigma_y/\sqrt{3}$.

P_o, the ultimate strength of the unstiffened girder, was computed using tension field theory.[2]

$$(\tau_{cr})_o = k_o \frac{\pi^2 E}{12(1-\nu^2)} \frac{1}{\beta^2} \tag{5}$$

$$\frac{V_o}{V_p} = \frac{(\tau_{cr})_o}{\tau_y} + \frac{\sqrt{3}}{2} \frac{1 - \frac{(\tau_{cr})_o}{\tau_y}}{\sqrt{1+\alpha^2}} \tag{6}$$

$$V_o = \left(\frac{V_o}{V_p}\right) V_p \tag{7}$$

$$P_o = 2 V_o \tag{8}$$

$(\tau_{cr})_o$ is the web buckling shear stress and k_o is the buckling coefficient for the unstiffened panel in pure shear with simply supported edges.

$$k_o = 5.34 + \frac{4.00}{\alpha^2} \text{ for } \alpha \geq 1 \quad (9)$$

$$k_o = 4.00 + \frac{5.34}{\alpha^2} \text{ for } \alpha \leq 1 \quad (10)$$

V_p is the plastic shear force calculated, assuming the web to be completely yielded, from $V_p = \tau_y A_w$.

2.4 Test Setup

The girders were tested in a hydraulic universal testing machine. As shown in Fig. 5 the girders were simply supported at their ends by rollers, and the load was applied at midspan. Load was transferred from the machine crosshead to a girder through a spherical bearing block which also supplied lateral bracing to the compression flange at this point.

Additional lateral bracing was provided at the quarter points by steel pipes (Fig. 5). The bracing was designed to permit sufficient vertical deflection of the girder by pinning the pipes to the girder as shown in Fig. 6.

Centerline deflection, end support settlements, lateral web deflections, and strains in the web and longitudinal and transverse stiffeners were measured as described in Chapter 3. Various instruments were used to obtain this information, and in addition, the girder was whitewashed so that the extent of yielding could be observed and photographed.

3. TEST PROCEDURE AND RESULTS

3.1 Introduction

In this chapter the testing procedure, general girder behavior and the test results are described in detail. The test results consist primarily of load-deflection curves, web deflection diagrams, plots of various types of strain gage data and the observed ultimate loads. In addition, photographs of the girders provide a visual indication of the locations and patterns of yielding which developed during the tests.

In the following discussion a coordinate system will be used to identify points of importance on the test girders. The origin is at the geometric center of the web of each specimen, with the x-axis in the longitudinal direction, the y-axis in the transverse direction, and the z-axis perpendicular to the plane of the web (see Nomenclature). The side of the girder in the positive z direction will be called the near side of the girder, and the side in the negative z direction will be referred to as the far side. Thus all the longitudinal stiffeners were on the near side, and all the transverse stiffeners were on the far side.

One end of Girder LS1 (the first test girder) had no longitudinal stiffener; the test on this part of LS1 was referred to as T1, a control test. The other half of this same girder had a longitudinal stiffener which made it stronger than the tested portion, and this end was tested

as LS1-T2, the second test on Girder LS1. A test on Girder LS2 investigated the effect of stiffener size, three tests on Girder LS3 checked the effect of aspect ratio, and two tests on LS4 investigated the effect of two stiffener locations different from that of LS1, LS2 and LS3.

3.2 General Test Procedure

The load-versus-center line deflection curves provide a convenient record of the testing history and general behavior for each girder. The ordinate for these curves (Figs. 7 to 10) is the applied load P, while the abscissa is the vertical deflection of a girder at midspan ($v_{\mathbb{L}}$). Measured with a dial gage mounted on the base of the testing machine, the center line deflection readings were used as a control on the testing speed and to indicate when the ultimate load had been reached. Scales mounted on the end bearing stiffeners were read with an engineer's level to determine the support settlements. These support settlements have been used to correct the center line deflection readings plotted in Figs. 7 to 10.

In the following description of the test procedure, Girder LS1 will be used as an example, and the P vs. $v_{\mathbb{L}}$ curve for this girder (Fig. 7) will be referred to frequently in the description. The numbered circles in Fig. 7 indicate positions on the curve where the loading was stopped and measurements taken. These positions are referred to by the load numbers next to the circles.

Testing of Girder LS1 was initiated by taking readings on all instruments at zero load (Load No. 1). Load was then applied gradually up to a predetermined level (Load No. 2) at which measurements again were made. This procedure was continued until inelastic behavior was observed, as indicated by a substantial increase in deflection per unit load (Load No. 6). When readings had been completed at this stage, the load was reduced to zero, completing the first load cycle. The purpose of this cycle was to eliminate the effects of residual stresses on strain gage readings in the second load cycle up to the maximum load of the first cycle.

The second load cycle, starting with Load No. 7, was initially carried out in the same manner as the first cycle, stopping at predetermined load levels at take the various measurements. In the inelastic range (Load Nos. 13 to 17), loading was stopped at selected deflection increments and allowed to stabilize while deflection was held constant. Readings were taken only after the load had stabilized so that they would be independent of the loading rate. When a substantial increase in deflection was observed with no accompanying increase in load, the ultimate load was obtained and load was removed from the girder (Load No. 18), completing test T1.

Failure occurred in test LS1-T1 in the three panels which were not longitudinally stiffened. The three panels with longitudinal stiffeners were not damaged at this stage. To permit a second test on these undamaged panels, the failed panels were reinforced by welding stiffeners along the tension diagonals. This repair is indicated on the

Testing of Girder LS1 was initiated by taking readings on all instruments at zero load (Load No. 1). Load was then applied gradually up to a predetermined level (Load No. 2) at which measurements again were made. This procedure was continued until inelastic behavior was observed, as indicated by a substantial increase in deflection per unit load (Load No. 6). When readings had been completed at this stage, the load was reduced to zero, completing the first load cycle. The purpose of this cycle was to eliminate the effects of residual stresses on strain gage readings in the second load cycle up to the maximum load of the first cycle.

The second load cycle, starting with Load No. 7, was initially carried out in the same manner as the first cycle, stopping at predetermined load levels at take the various measurements. In the inelastic range (Load Nos. 13 to 17), loading was stopped at selected deflection increments and allowed to stabilize while deflection was held constant. Readings were taken only after the load had stabilized so that they would be independent of the loading rate. When a substantial increase in deflection was observed with no accompanying increase in load, the ultimate load was obtained and load was removed from the girder (Load No. 18), completing test T1.

Failure occurred in test LS1-T1 in the three panels which were not longitudinally stiffened. The three panels with longitudinal stiffeners were not damaged at this stage. To permit a second test on these undamaged panels, the failed panels were reinforced by welding stiffeners along the tension diagonals. This repair is indicated on the

P vs. $v_{\mathbb{C}}$ curve by a weld symbol at Load No. 19 and is shown in detail in Fig. 11a. For Girders LS3 and LS4, as well as Girder LS1, this method of repair proved to be an excellent means of reinforcing damaged panels so that further tests of undamaged panels could be conducted.

The second test on Girder LS1 (Load Nos. 19 to 35) was conducted in a manner similar to that of the first test. At the end of test T2, the girder was subjected to a destruction test (Load Nos. 35 to 38) which was terminated after the load-carrying capacity was reduced by about ten percent. This destruction test was carried out only to observe the deformation capacity of the girder and thus the only readings taken after Load No. 35 were centerline deflection readings using an engineer's level and a scale mounted on the web at mid height.

The procedure used in testing Girders LS2, LS3 and LS4 was similar to that described above for Girder LS1. A record of the testing history of these girders is provided by their respective P vs. $v_{\mathbb{C}}$ curves (Figs. 8 to 10). The repairs for Girders LS3 and LS4 are shown in Fig. 11b, c and d. Since all six panels of Girder LS2 failed during the first test, a second test on this girder was not possible.

3.3 Behavior and Ultimate Loads

Girder LS1

There were two tests on Girder LS1. The first was a control test on the end of the girder which had three square panels with no longitudinal stiffeners. Between Load Nos. 13 and 14 (refer to Fig. 7)

yielding began along the tension diagonals, starting in the end panel. When Load No. 14 was reached, yielding was evident along the diagonals of all three panels, as shown in Fig. 12. This yielding became more pronounced by the time the ultimate load of 363.5 kips was reached. The girder was unloaded to zero kips at Load No. 18 to complete test T1.

The repairs (diagonal stiffeners) after test LS1-T1 are shown in Fig. 13, a photo taken after the destruction test. Test LS1-T2 began with Load No. 19, and the load-deflection curve (Fig. 7) indicates that the linear portion between Load Nos. 19 and 26 is steeper than the unloading line for test T1. This is the result of strengthening the failed panels with the diagonal repair stiffeners. For this test, as in test T1, the aspect ratio was 1.0, but a longitudinal stiffener was present at $\eta = 0.33$ in the test panels. Diagonal yield patterns formed as distinctly separate diagonals in the subpanels, as shown in Fig. 14, taken at Load No. 36. In the upper subpanels, horizontal and vertical yield lines formed. The ultimate load was 414.0 kips (Load No. 29). The appearance of the girder after the destruction test (Figs. 13 and 15) provide visual evidence of the effectiveness of the repair stiffeners on one end of the girder and the development of separate tension fields in the six subpanels at the other end of the girder.

Girder LS2

Girder LS2 had 4 in. x 1/2 in. longitudinal stiffeners in three square panels at one end and 5 1/2 in. x 1 in. stiffeners in the three square panels at the other end. The three panels with stronger stiffeners began yielding before the other three panels had failed, so only

one test was obtained from the specimen. Figure 16 shows the extent of yielding in the stronger end and Fig. 17 shows the weaker end at the same load (Load No. 18). In both figures separate tension diagonals in the subpanels are evident, with more pronounced yielding in the outermost panels. The ultimate load was 315.5 kips (Load No. 17). The appearance of the specimen after the destruction test is shown in Fig. 18.

Girder LS3

One end of Girder LS3 had two panels with α = 1.5 while the other end had four panels with α = 0.75. Throughout the girder length a continuous longitudinal stiffener was located at η = 0.33. Test T1 was conducted on the end panel with an aspect ratio of 1.5 and a 2 in. x 1/2 in. longitudinal stiffener. The ultimate load, 278.5 kips, was reached at Load No. 13 after the longitudinal stiffener had failed and the web had buckled through it. Figure 19 shows the buckled stiffener. After Load No. 15 this end panel was reinforced with a diagonal stiffener.

Test T2 was conducted on the other panel with α = 1.5. This panel had a 3 1/2 in. x 1/2 in. longitudinal stiffener. Again the horizontal and vertical yield line patterns were observed with tension diagonals forming in the lower subpanels (Fig. 20). The test was ended when extensive yielding had developed along the tension diagonals at an ultimate load of 296.0 kips (Load No. 21). The girder was unloaded and a diagonal stiffener was placed in the failed panel after Load No. 25.

In test LS3-T3 the four panels on the + x end of Girder LS3 had an aspect ratio of 0.75 and a longitudinal stiffener equal in size to that of LS3-T2 (3 1/2 in. x 1/2 in.). The ultimate load was 338.0 kips (Load No. 35). Figure 21 shows the yield patterns and deformations in the girder after the destruction test. The effectiveness of the repair stiffeners is again evident in this photo from the lack of yielding in the reinforced panels.

Girder LS4

The two halves of Girder LS4 were identical except that the longitudinal stiffener on one half was at $\eta = 0.2$ while on the other end it was at $\eta = 0.5$. Because of this single difference, it was not known which end would fail first. At the end of test T1 it was obvious that the end with $\eta = 0.5$ had failed; this occurred at an ultimate load of 380.5 kips (Load No. 18). Figure 22 shows the familiar yield patterns, and again the end panels had the most advanced yielding. This photo was taken at the end of test T1 (Load No. 19) after the girder was unloaded. Diagonal stiffeners were welded along the tension diagonals to prepare for test T2.

The stronger end of the girder with $\eta = 0.5$ reached its ultimate load at 405.5 kips (Load No. 28) when tension diagonals could be seen in all six subpanels. This is shown in Fig. 23, a photograph taken after the destruction test had been completed. As in the other tests, the effectiveness of the repair stiffeners and the development of separate tension diagonals in the subpanels are well documented in this photograph.

3.4 Web Deflections

Lateral web deflections were measured at selected cross sections in the test panels at various loads, using a special device designed for this purpose. This device consisted of a portable rigid truss to which dial gages were attached at certain y-coordinate points (Fig. 24). By placing the measuring device at various x-coordinate stations and reading the gages at the y-coordinates, the deflected configuration of a test panel was obtained. In tests LS1-T1 and T2, LS2-T1, and LS3-T1 and T2 web deflectionswere measured at the fifth-points (x-coordinates) of each panel. Measurements for LS3-T3 were made at the third-points of each panel, and for LS4-T1 and T2 they were made at the panel mid-points. Reference measurements on a milled steel surface were taken after each set of readings to check against accidental movement of the dial gages. Figures 25 to 32 show girder cross sections with the measured out-of-plane web deflection superimposed.

The web deflections, relative to the reference surface, were plotted at the various y-coordinate points and then connected with straight lines. Figure 28, a typical web deflection plot, shows deflected shapes for Load Nos. 7, 10, and 13 (0^k, 180^k, and 278.5^k). At x = - 140, there is a bulge or valley in the upper subpanel; at x = - 125, the valley is lower in the cross section and it is deeper; the valley is still lower in the x = - 110 cross section; and finally, at x = - 95 the valley has reached the tension flange. These valleys will be discussed later.

3.5 Web Strains

For LS1-T2 and LS2-T1 strain rosettes were placed in the end panels, one gage on each side of the web at the center of each of the two subpanels. Their purpose was to measure three strains, thereby making possible calculation of the principal strains and stresses and their inclinations.

Figures 33 and 34 show the results of such calculations for the various Load Nos. indicated. Tensile stresses are shown as arrows directed away from the point at which the gage was located, and compressive stresses are shown as arrows directed toward it. The solid arrows show measured strain results and the dashed arrows represent the stresses which were calculated from beam theory. A discussion of these figures and a comparison between measured and computed stresses is presented in Chapter 4.

3.6 Longitudinal and Transverse Stiffener Strains

Strains were measured on the longitudinal stiffeners midway between the transverse stiffeners. Four strain gages were located around the stiffeners as indicated in Fig. 35. On the transverse stiffeners, strains were measured midway between the longitudinal stiffener and the flanges, using the same locations as in Fig. 35. The purpose of these measurements was to provide a means of estimating the axial forces carried by the stiffeners.

It has been shown that an effective width of about twenty thicknesses of the web acts along with the stiffener in resisting lateral bending.[9] Using this information the location of the neutral axis at Section A-A (Fig. 36) has been calculated and used to separate analytically axial strains from transverse bending strains.

Axial strains calculated in this manner are plotted as abscissas and static loads as ordinates in Figs. 37 to 42. Each plotted point is marked by its corresponding load number to indicate the corresponding position on the load-deflection curve. Superimposed on these plots are the theoretical elastic load-strain curves calculated using beam theory by $\epsilon_b = \frac{M_x y}{EI}$, where M_x is the bending moment at the longitudinal location where strains were measured and y is the location of the stiffener above the neutral axis of the girder cross section. These beam theory strains represent the strains due to bending in the plane of the web.

Axial transverse stiffener strains were obtained by averaging the four strain gage results. These average axial strains have been plotted as abscissas and static loads as ordinates in Figs. 43 to 47.

4. DISCUSSION

4.1 Ultimate Loads

The measured experimental ultimate loads (P_u^{ex}) and the reference loads are given in Table 5. In order to compare these with theoretical values, ratios of P_u^{ex} to the reference loads were calculated; these are listed in the last three columns of Table 5. Since web buckling theory was used in computing P_{cr}, it is obvious from the high P_u^{ex}/P_{cr} ratios that this theory underestimates the shear strength of a panel considerably.

The beam theory yield load P_y does not provide an accurate prediction of the shear strength either, judging by the values of P_u^{ex}/P_y in Table 5. The distribution of stresses in a panel subjected to high shear is radically different from that assumed in beam theory because of the large lateral web deflections which develop.

The ultimate shear strength of a transversely stiffened plate girder was studied by Basler.[2] Using Basler's theory, P_o has been calculated for the test girders ignoring the presence of the longitudinal stiffener. Thus the P_u^{ex}/P_o values listed in Table 5 indicate the increase in shear strength due to the longitudinal stiffener for each test. In test LS1-T1 no longitudinal stiffener was present and the P_u^{ex}/P_o ratio shows experimental agreement with Basler's theory within 3%. For the other tests, the static shear strength was increased from 6% to 29% with an average increase of 17%. Clearly, the longitudinal stiffeners added considerably to the shear strengths of the test girders.

4.2 Lateral Web Movement

The results of lateral web deflection measurements have been presented for the end panel of each test (Figs. 25-32) because these panels yielded first despite the lower bending moment present. Comparing the deflected web shape in LS1-T1 (no longitudinal stiffener) to the other plots, it is obvious that the longitudinal stiffener considerably controlled the web movement in all cases. This was accomplished by the stiffener forcing a nodal point in the deflected shape of the web at the stiffener location. Only in LS3-T1 was there no such nodal point; in this case the longitudinal stiffener buckled before the girder failed. Figure 19 shows the extent of the buckling; a string is mounted along the length of the stiffener for comparison purposes.

The web deflection plots show deflection valleys along the tension diagonals of the panels. In Fig. 25 the valley can be traced from the upper left corner to the lower right corner of the panel. In Fig. 28 the valley also crosses the entire panel as it does in the previous case with no longitudinal stiffener; however, this happened because the stiffener buckled. In all of the other tests the longitudinal stiffener forced separate valleys to form in the subpanels. The largest web deflections were always observed in the larger subpanels near the center and along the diagonal valleys.

The longitudinal stiffener usually forced the web gradually toward the far side of the girder, that is, away from the side with the longitudinal stiffener.

4.3 Principal Stresses in Web Subpanels

As shown in Figs. 33-34 the principal stresses indicate a tension and a compression diagonal in each subpanel, The tensile stress increased as load increased. However, the compressive stress did not increase beyond the value developed when the web buckled along the compression diagonal. The valleys previously discussed are the observable results of this plate buckling.

For the loads plotted in Figs. 33-34 the upper subpanels had not yet reached their limit in carrying increasingly greater compressive stresses; by virtue of their smaller depth the upper subpanels were considerably stronger than the lower subpanels.

4.4 Stiffener Strains

Figures 37-42 show axial strain in the longitudinal stiffeners as a function of the load applied to the girder at midspan. Figures 43-47 show the same information for the transverse stiffeners.

From the longitudinal stiffener strain plots, it is evident that in all cases with the longitudinal stiffener above the neutral axis, the segment of the stiffener in the end panel carried greater axial force than in the other panels. The force in the longitudinal stiffener is composed of two parts: the horizontal component of the tension field force[6] and part of the horizontal force resisting bending moment in the section.

The refinement used in locating the neutral axis of the longitudinal stiffener section (Sect. 3.6) resulted in good agreement between theoretical elastic strains (calculated using beam theory) and the experimental strains up to 90% of the ultimate load. There was no agreement in the case where the longitudinal stiffener buckled prematurely (Fig. 39, LS3-T1). The cause of disagreement in LS3-T2 (Fig. 39) has not been definitely established, but it possibly is due to large deflections incurred in the interior panel during LS3-T1 when the stiffener segment in the exterior panel buckled. It is also possible that the boundary conditions imposed in T2 by the diagonal stiffener repair after T1 caused the deviation.

Figures 43-47 show that in all cases the transverse stiffener carried little or no axial force (indicated by axial strain in the plots) until at least 90% of the ultimate load was attained.

5. CONCLUSIONS

From the experimental work on four longitudinally stiffened plate girders described in this report, the following conclusions can be formulated:

1. Neither web buckling theory nor beam theory can be used to predict the shear strength of longitudinally stiffened plate girders.
2. The longitudinally stiffeners increased the shear strength of the test girders from 6 to 38%.
3. The longitudinal stiffeners were very effective in controlling lateral web deflections.
4. Because of the control of web deflections by the longitudinal stiffeners, separate tension fields were developed in the subpanels.
5. The shear strength of the longitudinally stiffened panels was attained only after the development of the tension fields.
6. The addition of diagonal repair stiffeners strengthened the failed panels so that no further yielding occurred in the repaired panels as a result of continued testing on other panels.

6. NOMENCLATURE

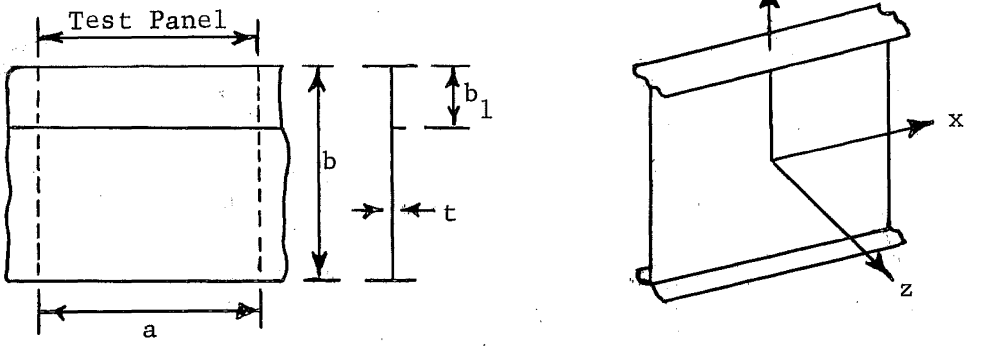

a	panel length
b	web depth
b_1	distance from top flange to center of longitudinal stiffener
k_o	web buckling coefficient for unstiffened panel
k^*	web buckling coefficient for longitudinally stiffened panel
t	web thickness
v	deflection in the negative y - direction
w	deflection in the positive z - direction
x,y,z	cartesian coordinate axes
E	modulus of elasticity (29, 600 ksi)
P	applied load
P_{cr}	theoretical web buckling load
P_o	theoretical ultimate load for girder without longitudinal stiffener
P_u^{ex}	experimentally obtained ultimate load

P_y	load which causes yielding at the neutral axis according to beam theory
V	shear force
α	aspect ratio, a/b
β	slenderness ratio, b/t
ϵ_y	yield strain, σ_y/E
η	longitudinal stiffener position, b_1/b
ν	Poisson's Ratio (0.3)
σ_y	yield stress, $\epsilon_y E$
τ_y	yield stress in shear, $\sigma_y/\sqrt{3}$

7. TABLES AND FIGURES

Test	$\epsilon_y=\sigma_y/E$	α	β	η	Longitudinal Stiffeners	Transverse Stiffeners
LS1-T1	0.00158	1.0	256	---	none	3"x3/4"
LS1-T2	0.00158	1.0	256	0.33	4"x1"	3"x3/4"
LS2-T1	0.00133	1.0	275	0.33	4"x1/2"	3"x3/4"
LS3-T1	0.00129	1.5	276	0.33	2"x1/2"	5"x3/8"
LS3-T2	0.00129	1.5	276	0.33	3 1/2"x1/2"	5"x3/8"
LS3-T3	0.00129	0.75	276	0.33	3 1/2"x1/2"	5"x1/2"
LS4-T1	0.00164	1.0	260	0.20	3 1/2"x1/2"	3"x1/2"
LS4-T2	0.00164	1.0	260	0.50	3 1/2"x1/2"	4 1/2"x1/2"

Table 1 Test Parameters

SPECIMEN	LS1		LS2	LS3			LS4	
TEST	T1	T2	T1	T1	T2	T3	T1	T2
Comp. Flg.								
Width	14.12		14.12	14.24			14.12	
Thickness	1.498		1.494	1.516			1.511	
Tens. Flg.								
Width	14.10		14.12	14.20			14.22	
Thickness	1.497		1.503	1.516			1.508	
Web								
Depth*	50.0		50.0	50.0			50.0	
Thickness	0.195		0.182	0.181			0.192	
Long. Stiff.								
Width	---	4.04	3.97 5.52	1.97	3.44	3.44	3.47	3.50
Thickness	---	1.016	0.500 1.006	0.502	0.511	0.510	0.511	0.511
Trans. Stiff.								
Width*	3.0	3.0	3.0	5.0	5.0	5.0	3.0	4.50
Thickness*	0.75	0.75	0.75	0.375	0.375	0.50	0.50	0.50

* Nominal Sizes

Table 2 Average Plate Dimensions

Specimen	Component	σ_y (ksi)	% Elong. (in 8 in.)	Chemical Composition			
				C	Mn	P	S
LS1	Comp. Flg.	30.5	33.8	0.20	1.11	0.009	0.022
	L.S.	30.6	30.3				
	Web*	46.8	23.8	0.19	0.53	0.010	0.021
	Tens. Flg.	30.2	34.7	0.20	1.11	0.009	0.022
LS2	Comp. Flg.	29.4	33.4	0.20	1.11	0.009	0.022
	L.S.(4x½)	39.8	28.9				
	L.S.(5½x1)	29.0	31.0				
	Web*	39.4	29.0	0.16	0.58	0.010	0.024
	Tens. Flg.	30.0	35.0	0.20	1.11	0.009	0.022
LS3	Comp. Flg.	29.8	33.0	0.20	1.11	0.009	0.022
	L.S.(2x½)	39.2	26.9				
	L.S.(3½x½)	35.8	29.7				
	Web*	38.2	28.6	0.19	0.53	0.010	0.021
	Tens. Flg.	29.5	35.5	0.20	1.11	0.009	0.022
LS4	Comp. Flg.	30.5	34.5	0.20	1.11	0.009	0.022
	L.S.(3½x½)T1	36.0	28.6				
	L.S.(3½x½)T2	36.3	29.3				
	Web*	48.6	23.0	0.19	0.53	0.010	0.021
	Tens. Flg.	30.0	31.5	0.20	1.11	0.009	0.022

* Web values are average values from the two tensile specimens (Maximum difference between the two yield stresses was 1.4 ksi)

Table 3 Material Properties

Specimen	Test	k*	P_{cr} (kips)	P_y (kips)	P_o (kips)
LS1	T1	9.34	74.3	523.6	351.5
	T2	15.9	126.6	514.6	351.5
LS2	T1	15.9	102.4	408.7	276.9
LS3	T1	13.7	87.1	396.0	215.1
	T2	13.7	87.1	394.7	215.1
	T3	19.0	120.8	394.7	302.7
LS4	T1	12.3	93.4	531.8	357.7
	T2	25.4	193.0	536.2	357.7

Table 4 Reference Loads

Test	P_u^{ex} (kips)	P_u^{ex}/P_{cr}	P_u^{ex}/P_y	P_u^{ex}/P_o
LS1-T1	363.5	4.89	0.69	1.03
LS1-T2	414.0	3.27	0.80	1.18
LS2-T1	315.5	3.08	0.77	1.14
LS3-T1	278.5	3.20	0.70	1.29
LS3-T2	296.0	3.40	0.75	1.38
LS3-T3	338.0	2.80	0.86	1.12
LS4-T1	380.5	4.07	0.72	1.06
LS4-T2	405.5	2.10	0.76	1.13

Table 5 Test Results

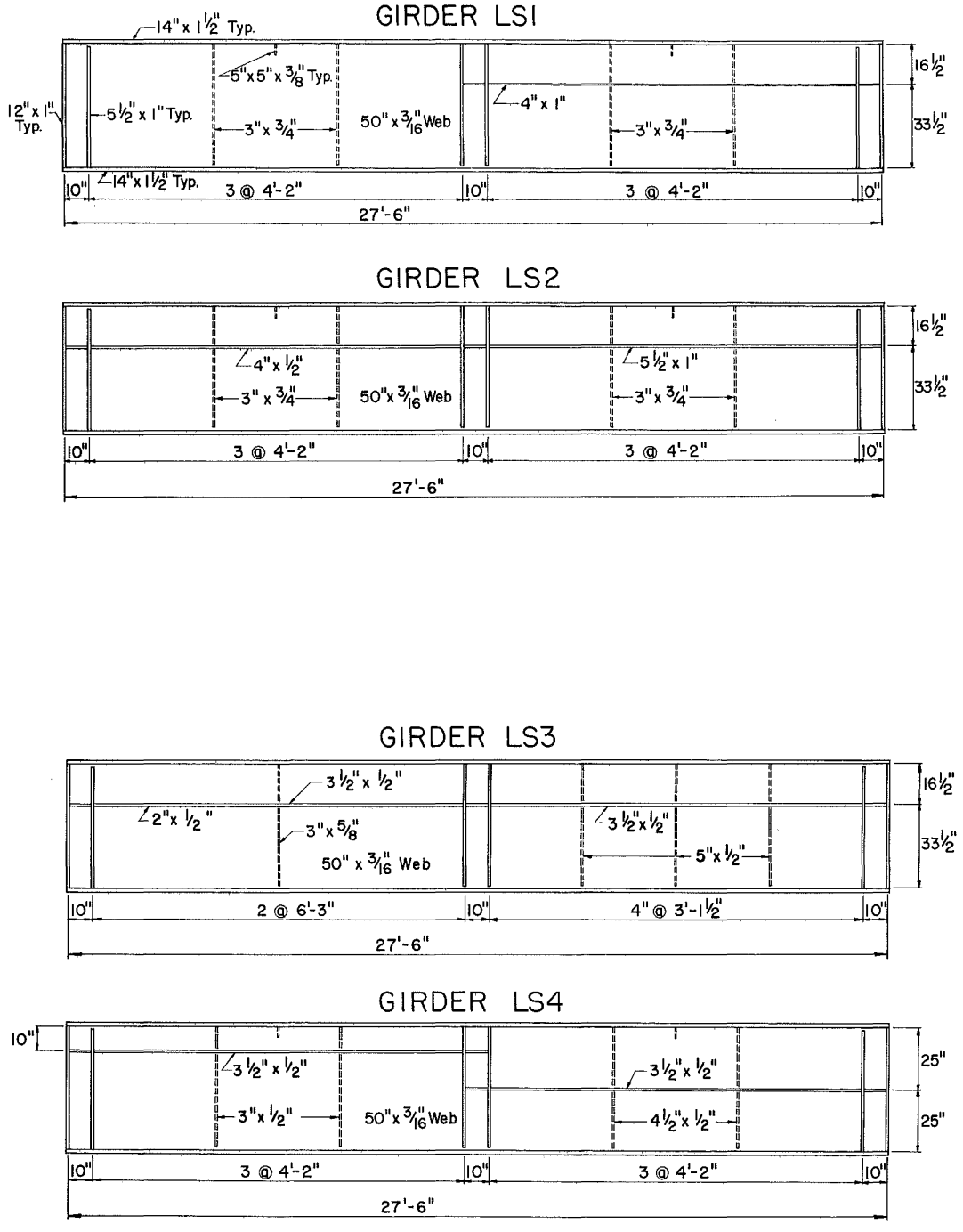

Fig. 1 Test Girders

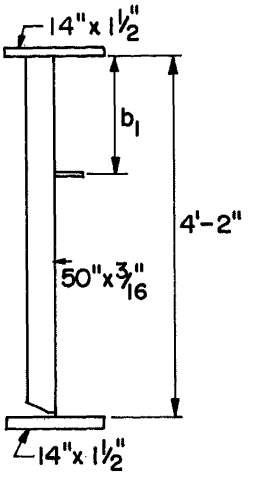

Fig. 2 Typical Cross Section

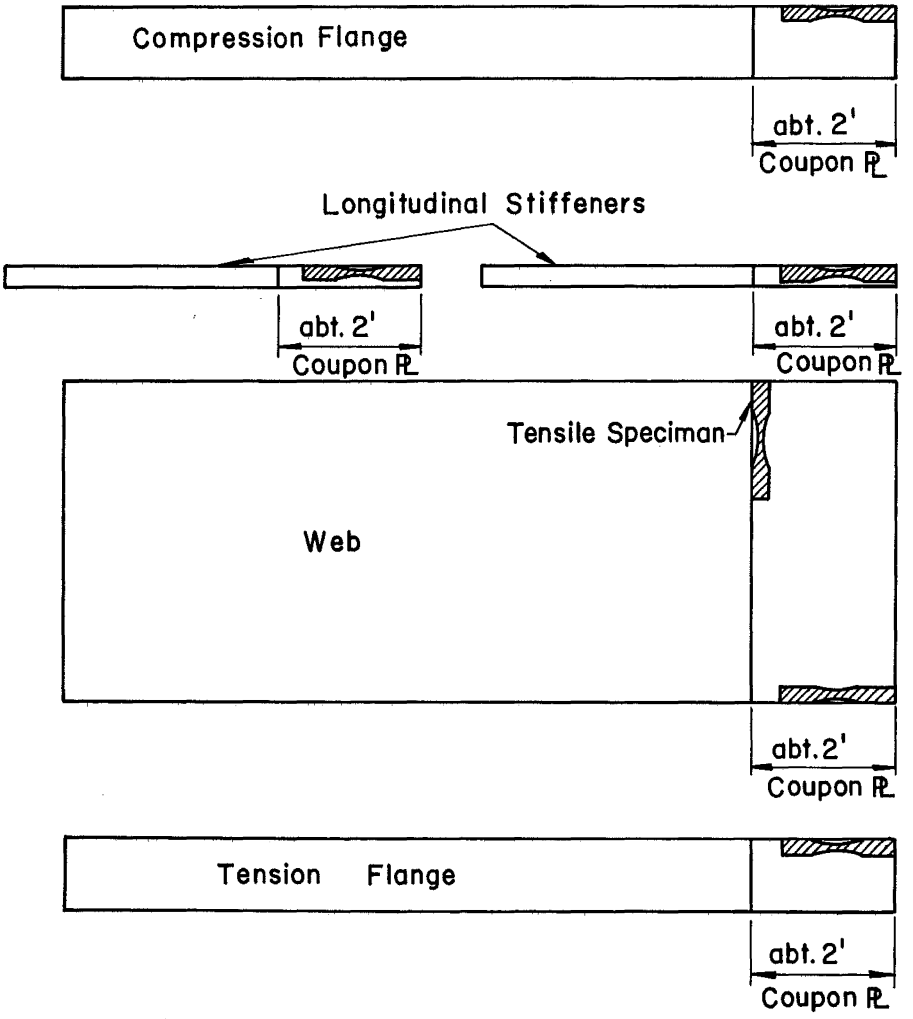

Fig. 3 Locations of Coupon Plates and Tensile Specimens

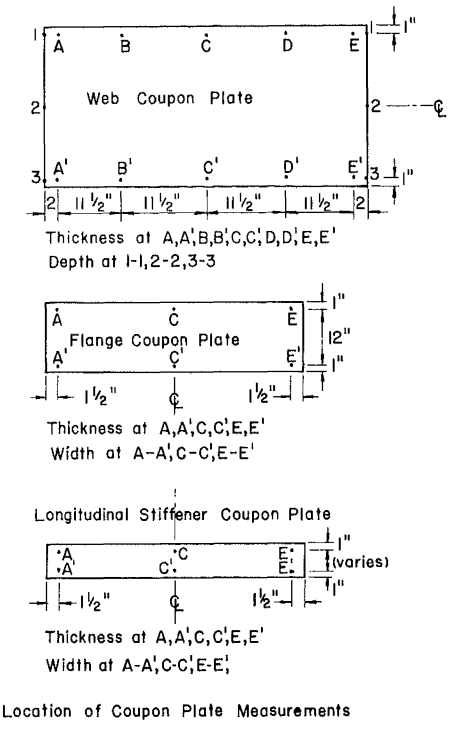

Fig. 4 Location of Coupon Plate Measurements

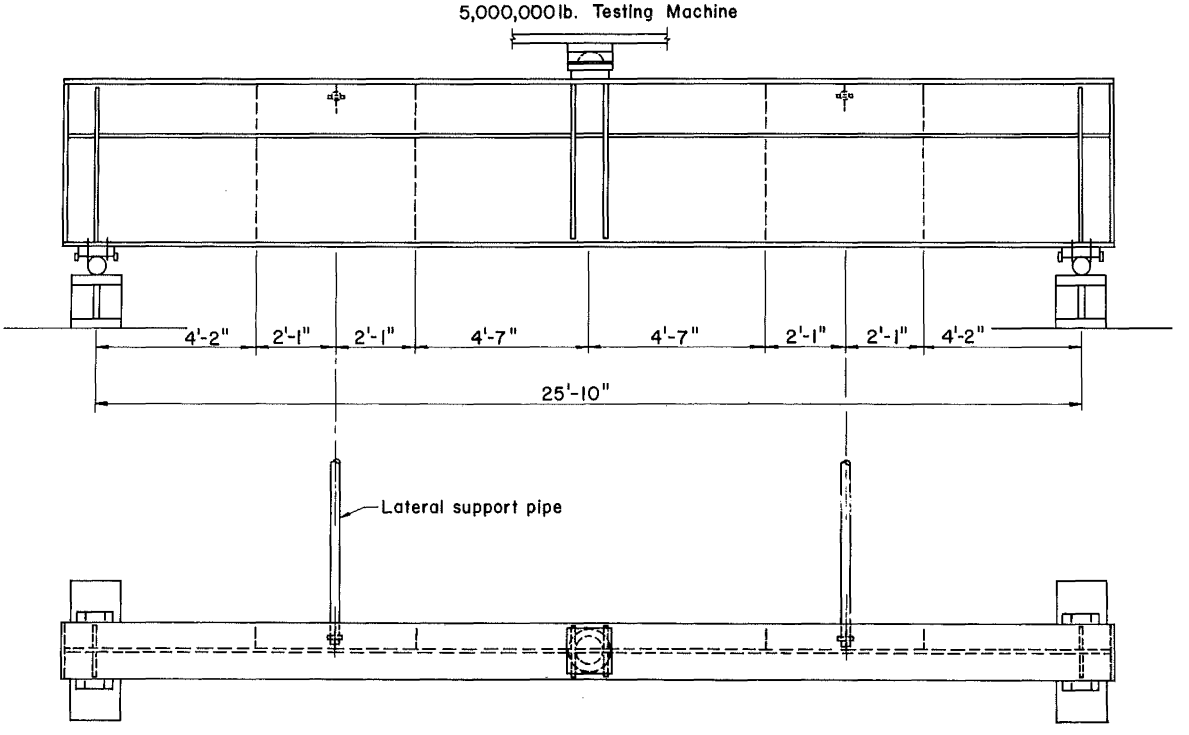

Fig. 5 Test Setup

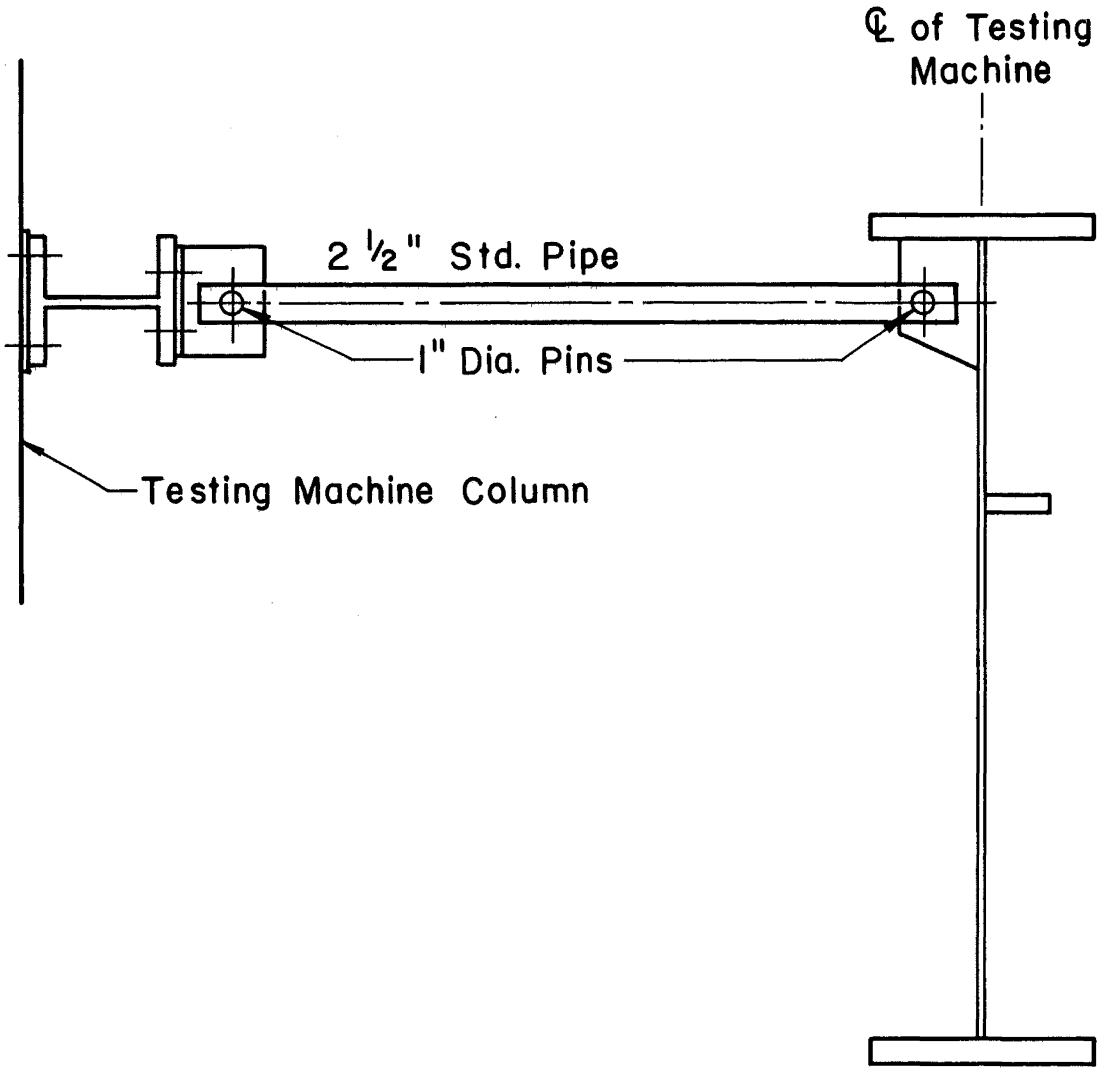

Fig. 6 Section at Lateral Support Pipe

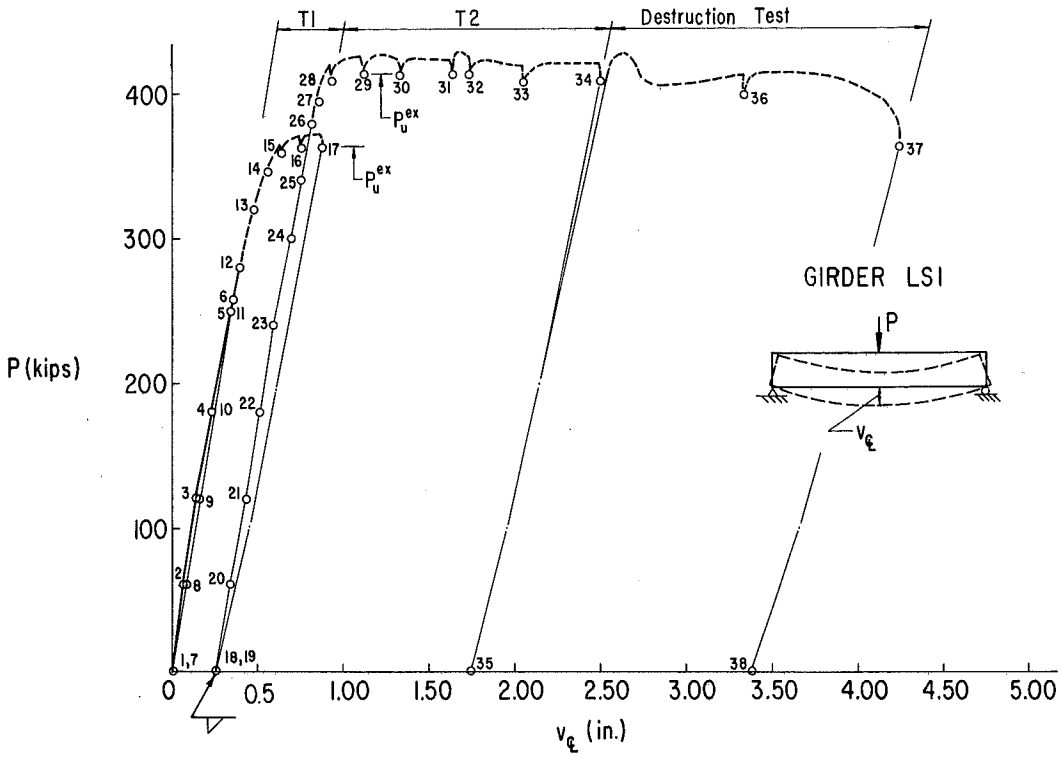

Fig. 7 Load-Vs- Centerline Deflection Curve for Girder LS1

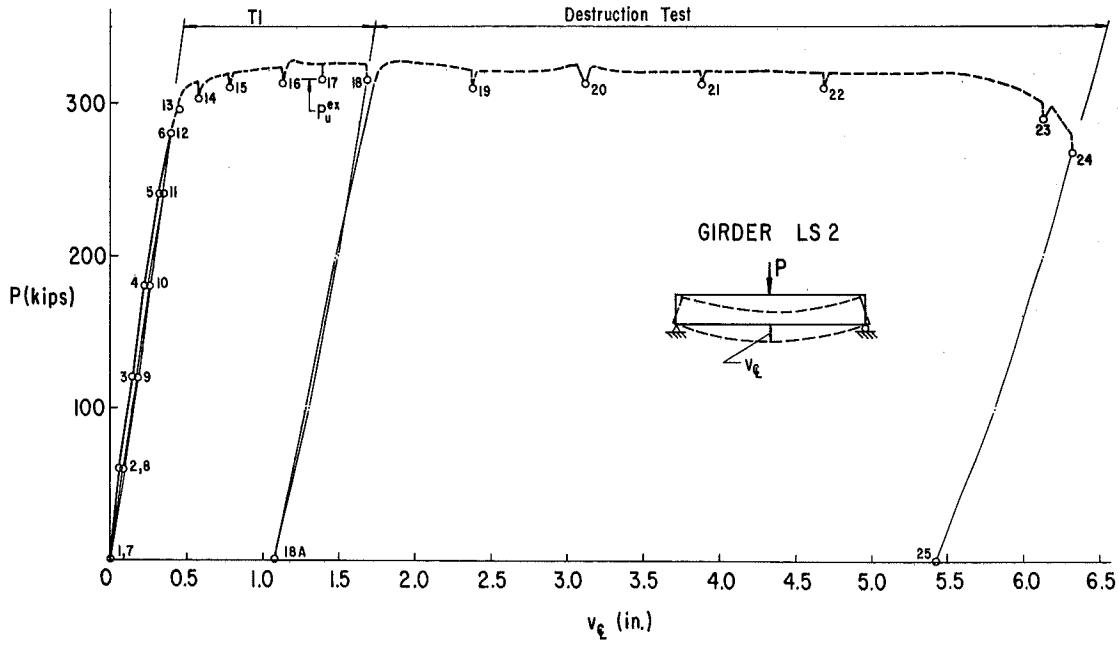

Fig. 8 Load-Vs-Centerline Deflection Curve for Girder LS2

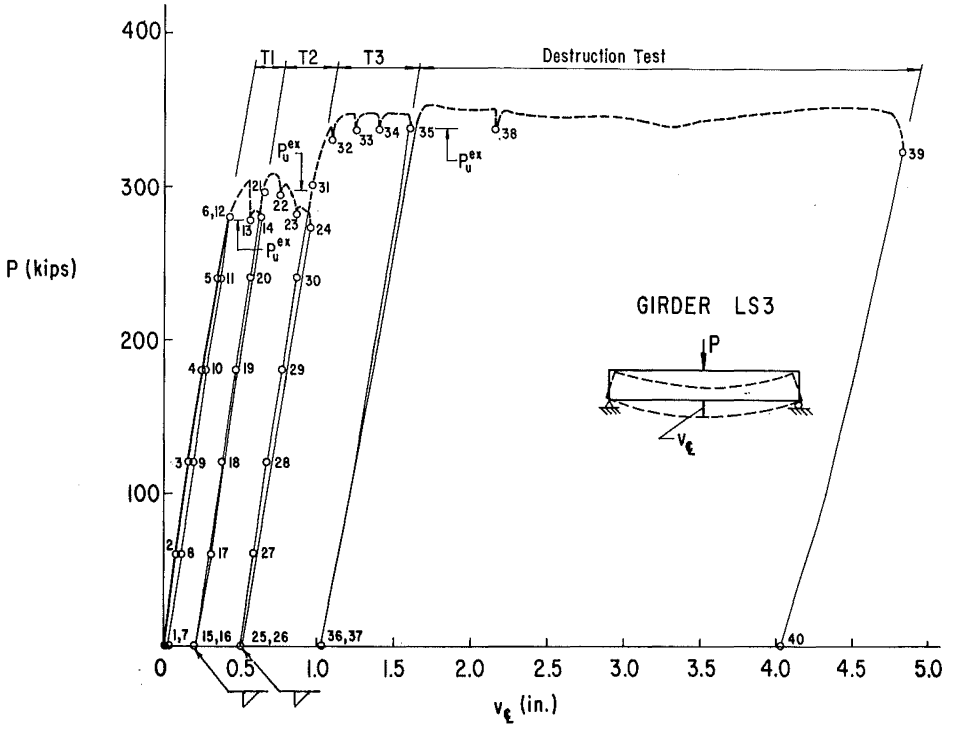

Fig. 9 Load-Vs-Centerline Deflection Curve for Girder LS3

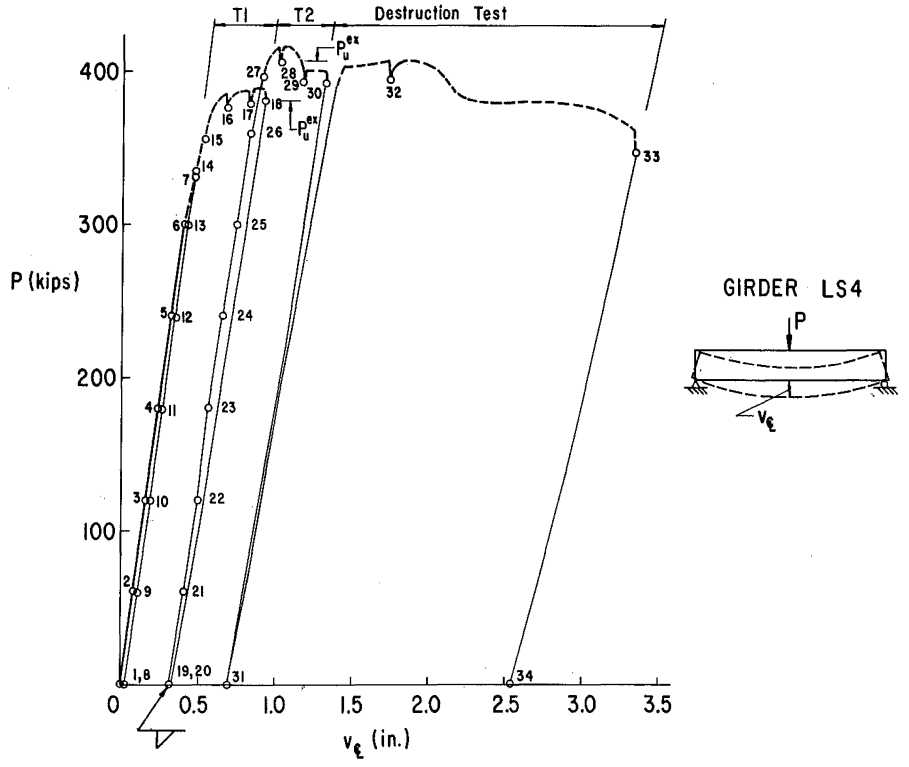

Fig. 10 Load-Vs-Centerline Deflection Curve for Girder LS4

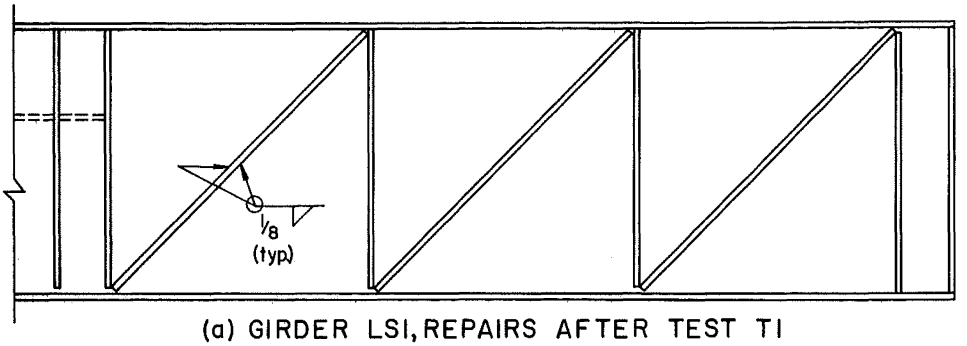

(a) GIRDER LSI, REPAIRS AFTER TEST TI

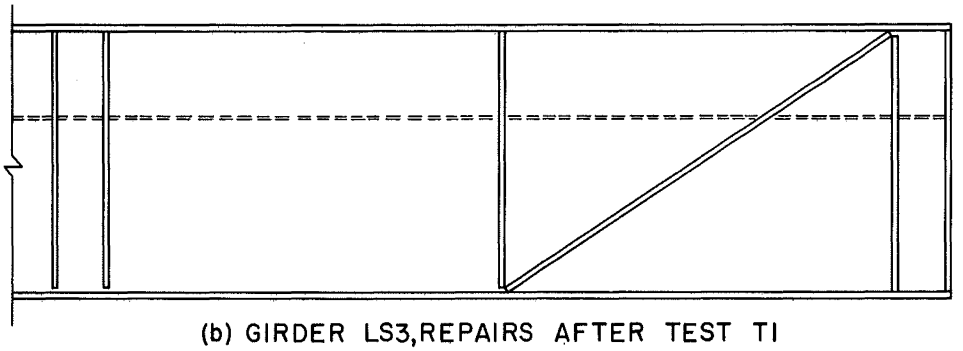

(b) GIRDER LS3, REPAIRS AFTER TEST TI

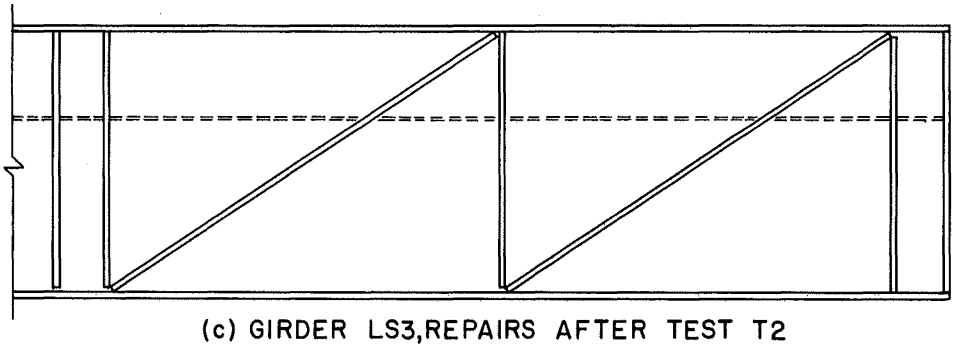

(c) GIRDER LS3, REPAIRS AFTER TEST T2

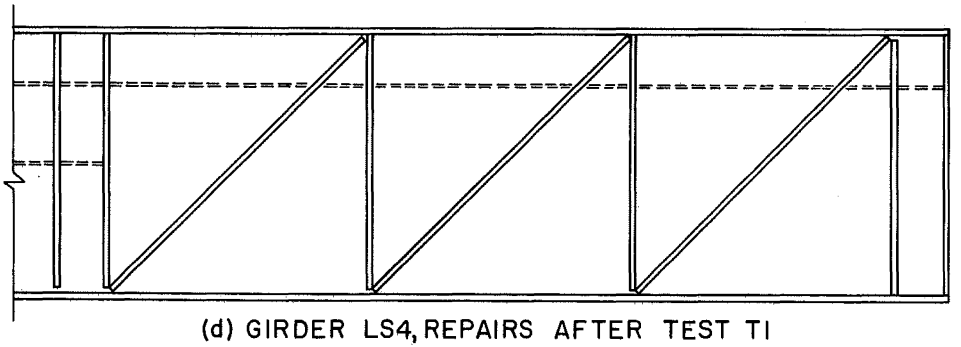

(d) GIRDER LS4, REPAIRS AFTER TEST TI

NOTE: ALL REPAIR STIFFENERS WERE CUT FROM 6" x ½" MILD STEEL BARS AND FITTED TO THE DEFORMED SHAPE OF THE WEB BEFORE BEING WELDED INTO PLACE.

Fig. 11 Repairs of Failed Panels

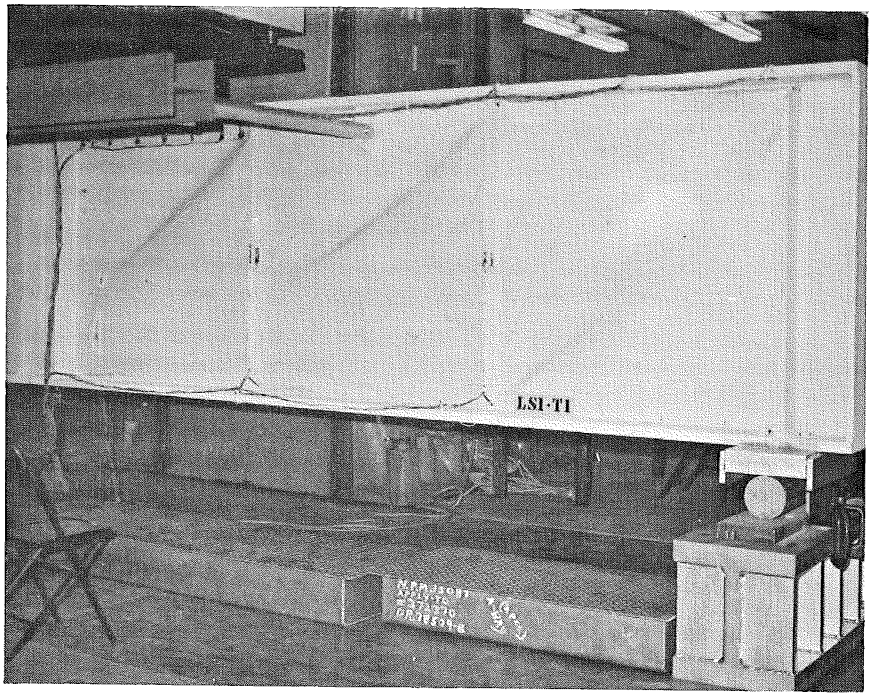

Fig. 12 Yield Patterns in Girder LS1 at Load No. 14

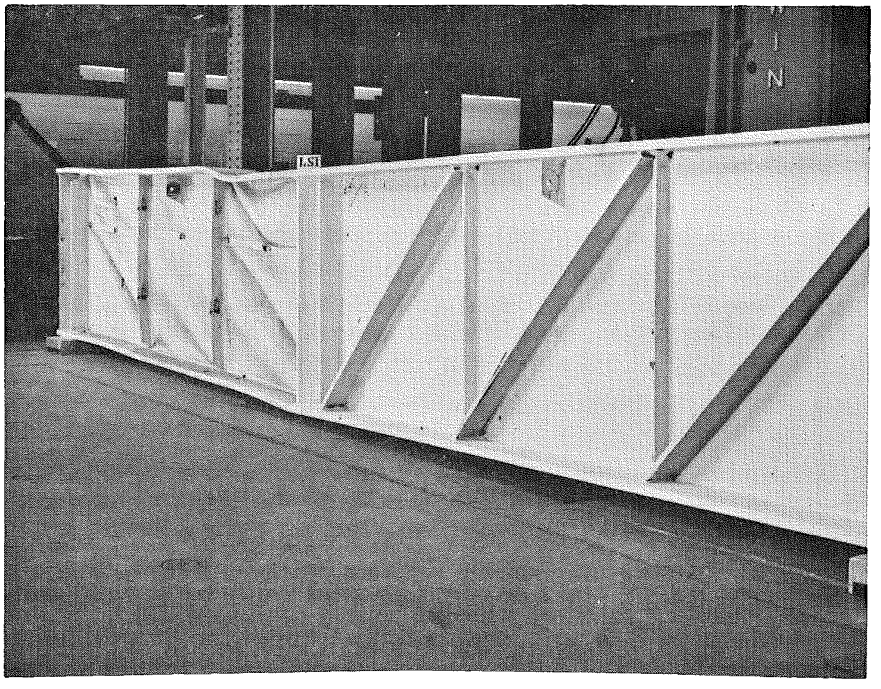

Fig. 13 Girder LS1 After Destruction Test (far side)

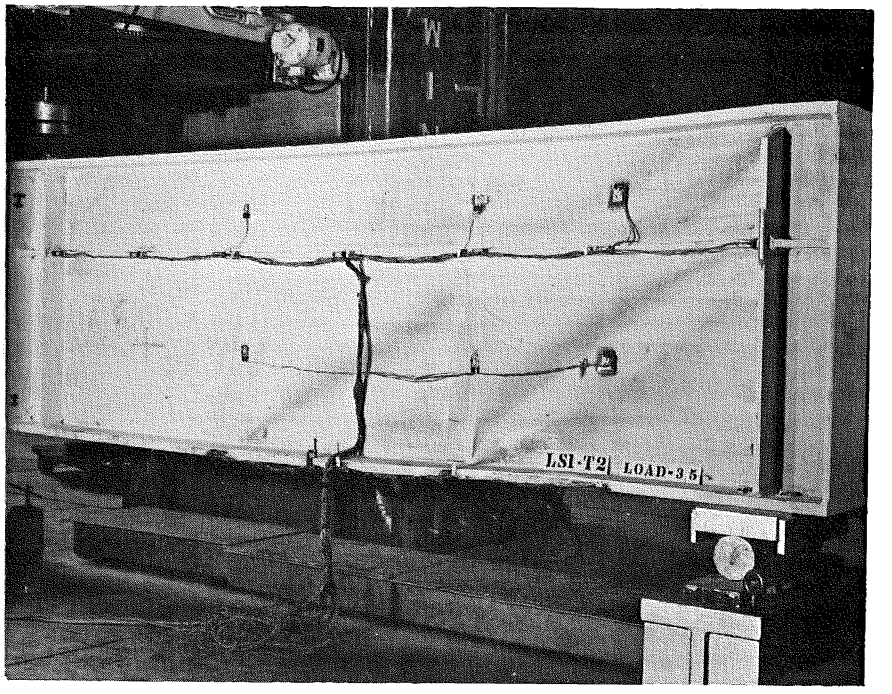

Fig. 14 Appearance of Girder LS1 at Load No. 35

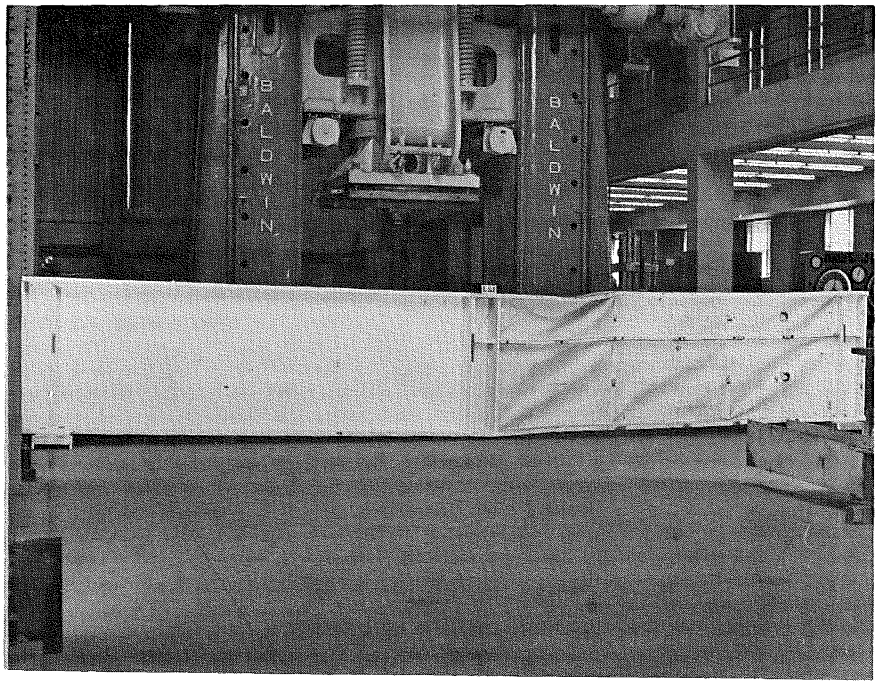

Fig. 15 Girder LS1 after Destruction Test (near side)

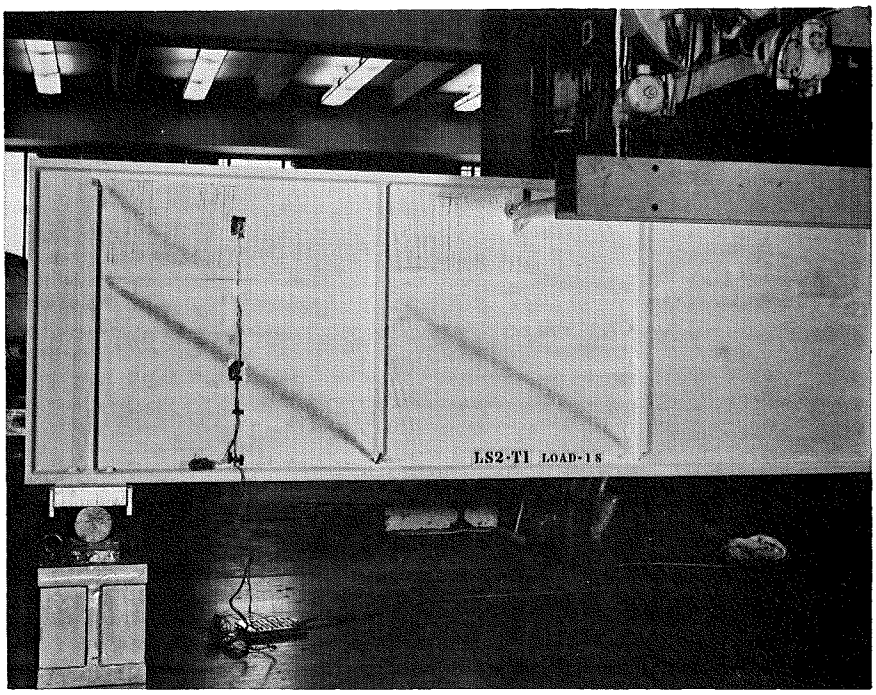

Fig. 16 Girder LS2 at Load No. 18 (+ x end)

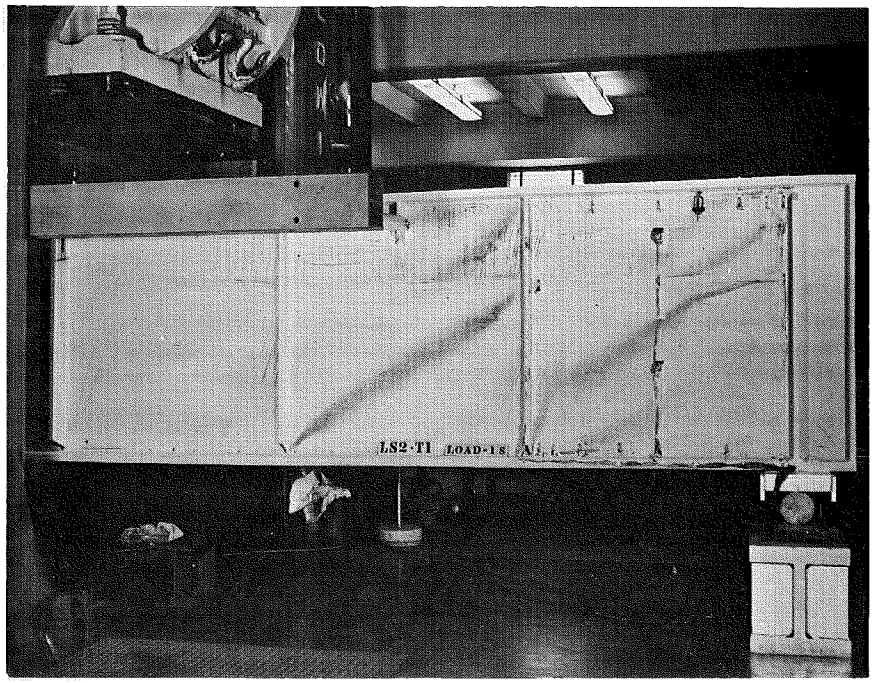

Fig. 17 Girder LS2 at Load No. 18 (- x end)

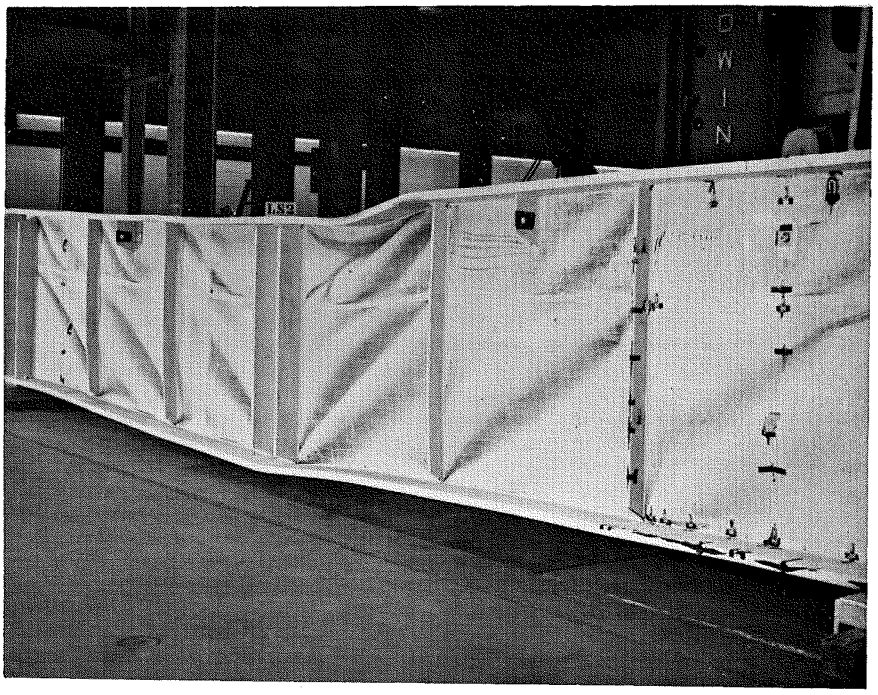

Fig. 18 Girder LS2 after Destruction Test

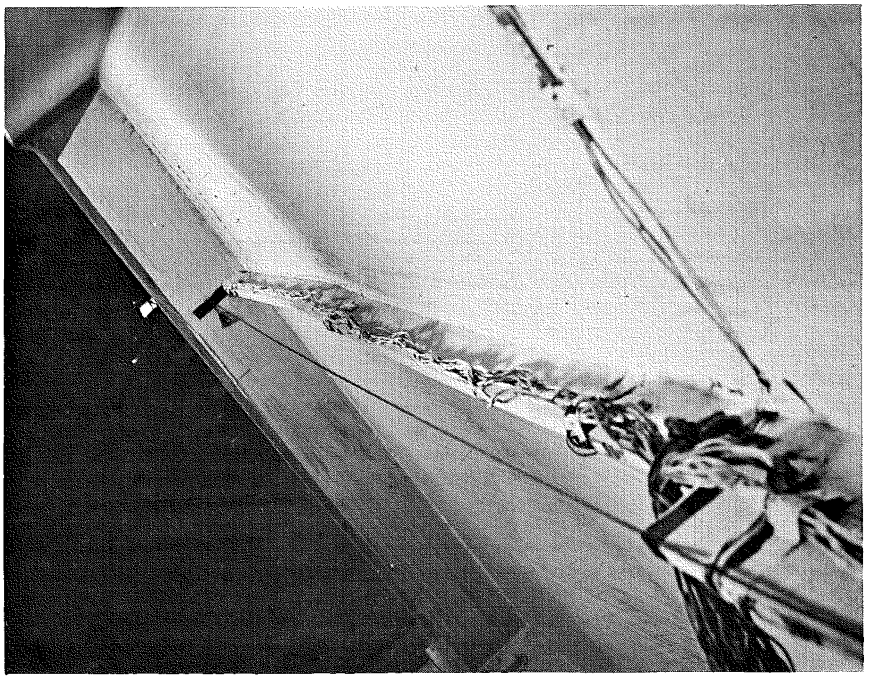

Fig. 19 Buckled Longitudinal Stiffener in Girder LS3 after Test T1

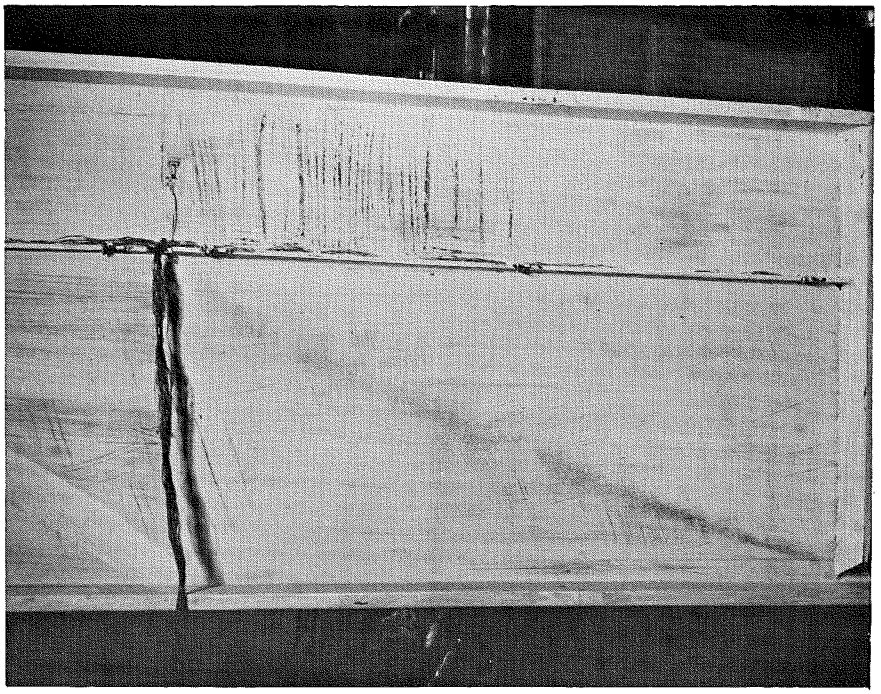

Fig. 20 Test Panel of Girder LS3 after Test T2

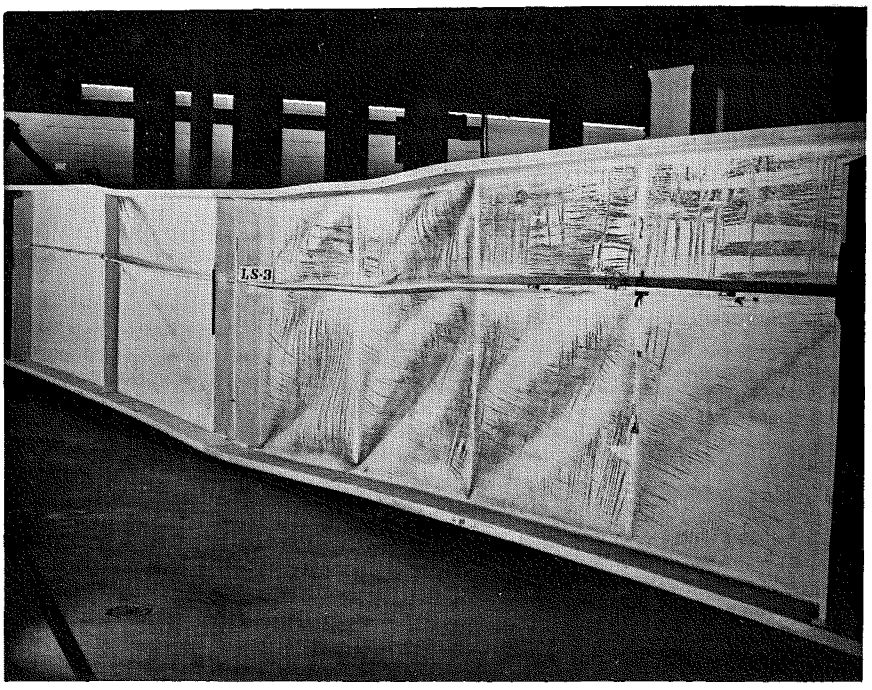

Fig. 21 Girder LS3 after Destruction Test

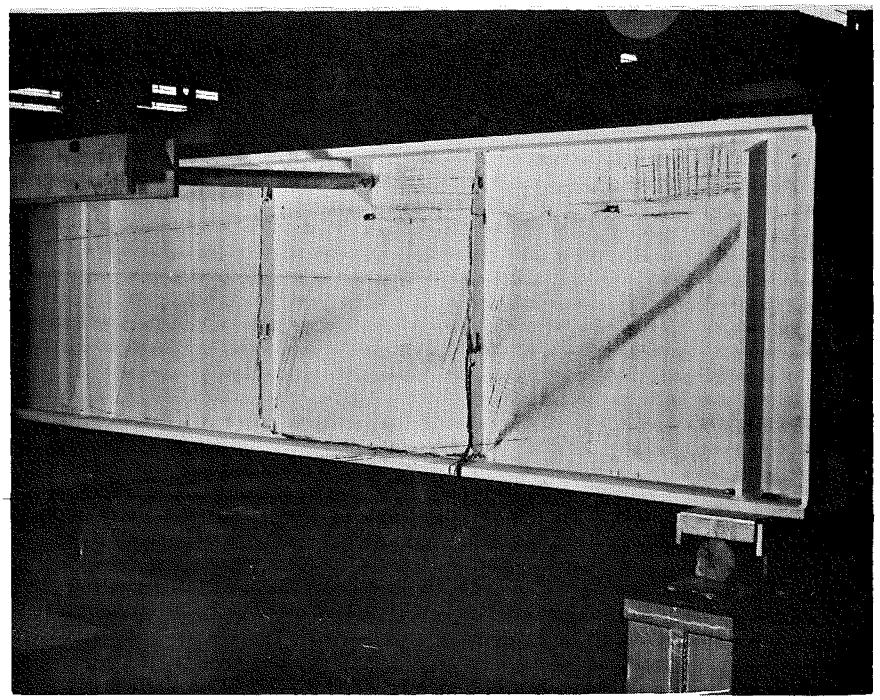

Fig. 22 Yield Patterns in Girder LS4 at Load No. 18

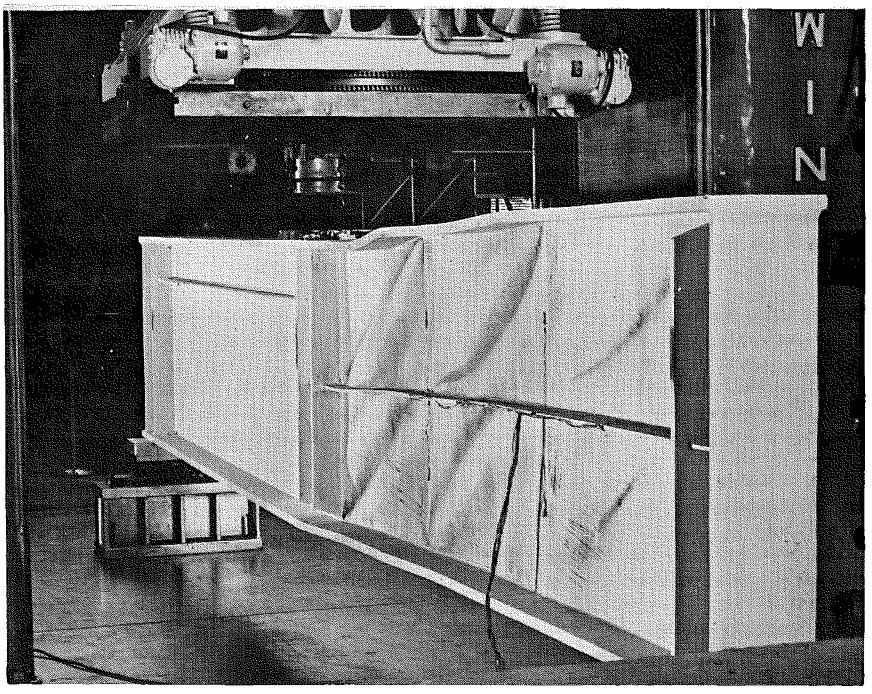

Fig. 23 Girder LS4 after Destruction Test

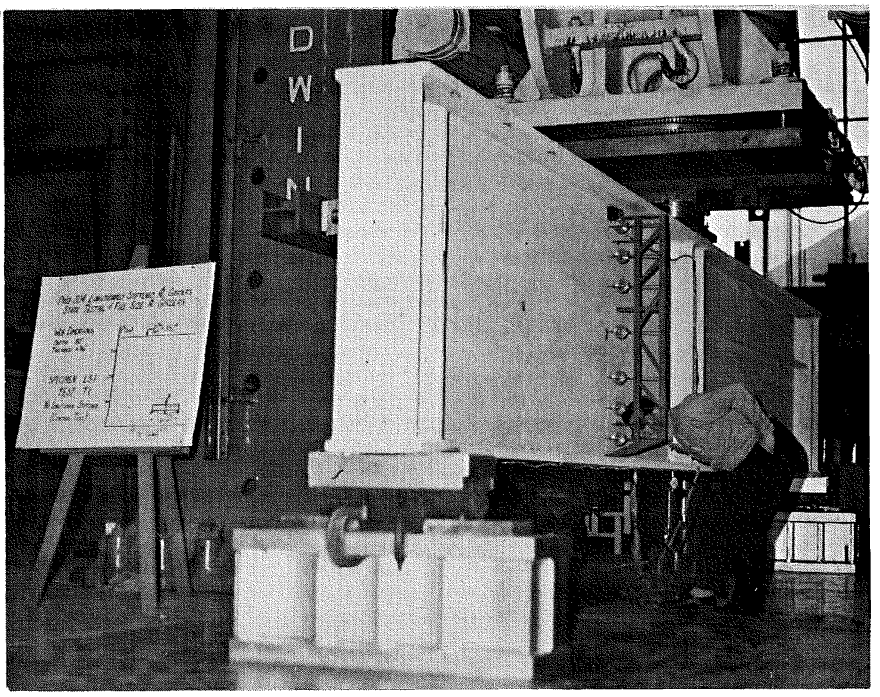

Fig. 24 Web Deflection Dial Gage Rig in Use

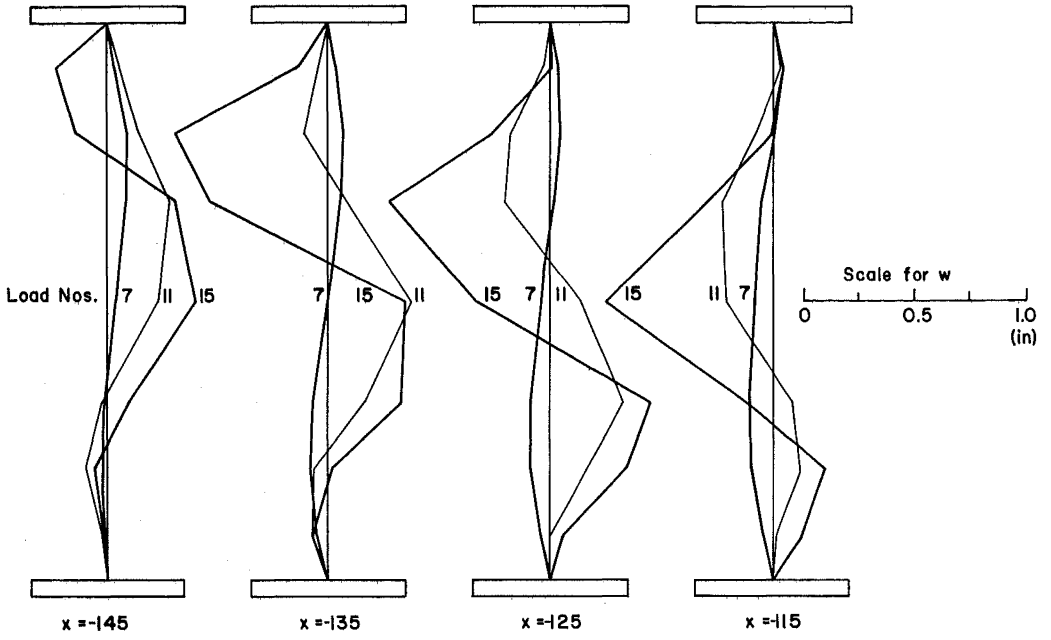

Fig. 25 Web Deflections (Test LS1-T1)

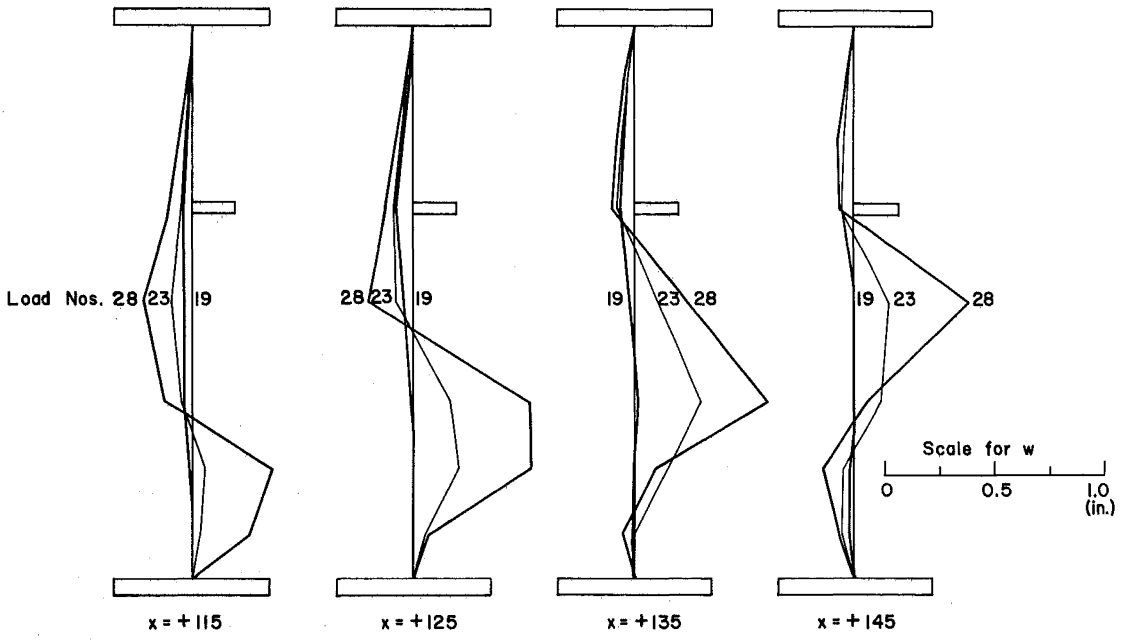

Fig. 26 Web Deflections (Test LS1-T2)

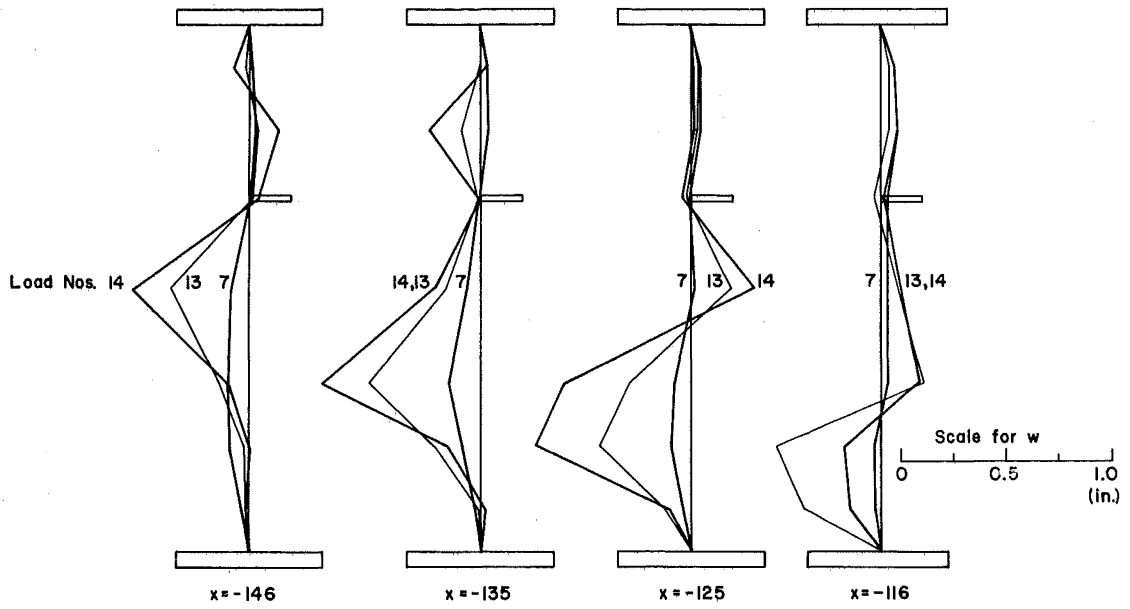

Fig. 27 Web Deflections (Test LS2-T1)

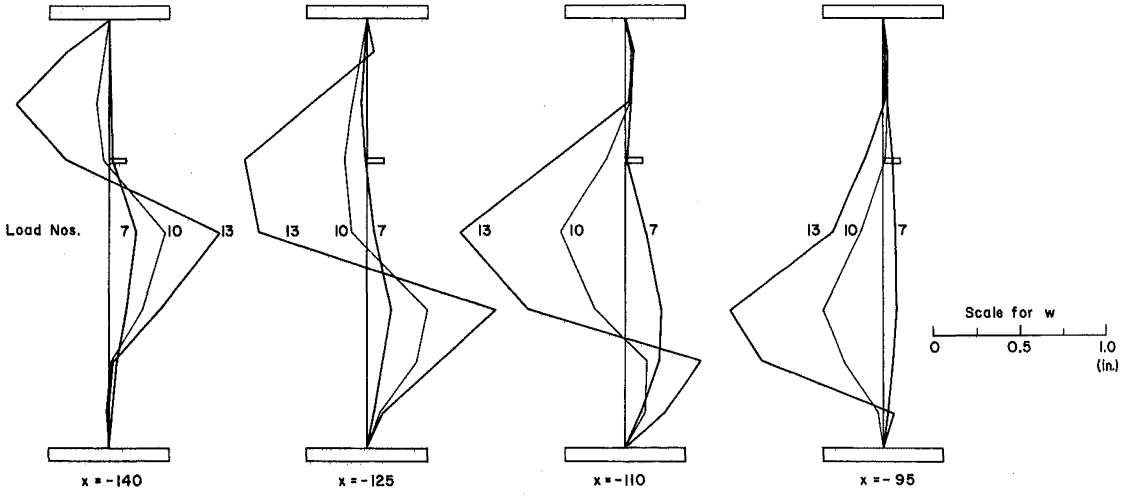

Fig. 28 Web Deflections (Test LS3-T1)

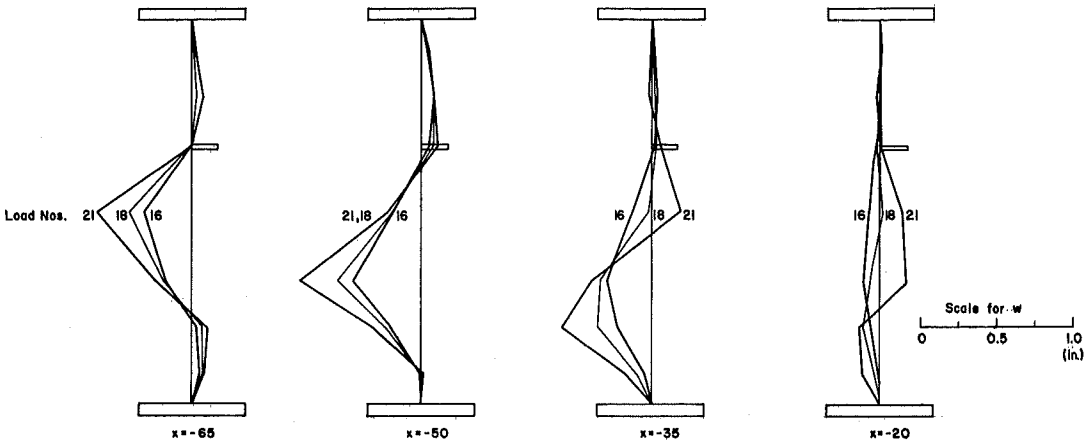

Fig. 29 Web Deflections (Test LS3-T2)

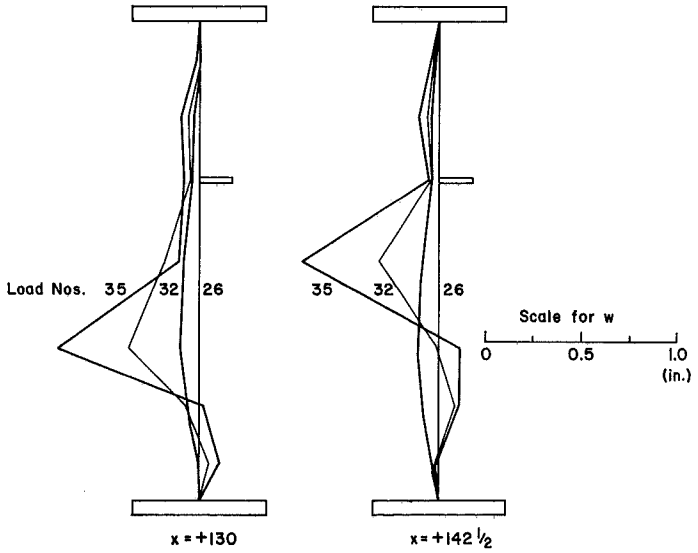

Fig. 30 Web Deflections (Test LS3-T3)

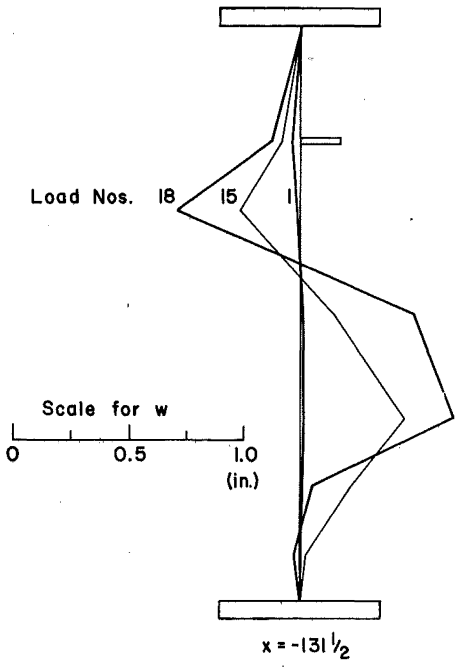

Fig. 31 Web Deflections (Test LS4-T1)

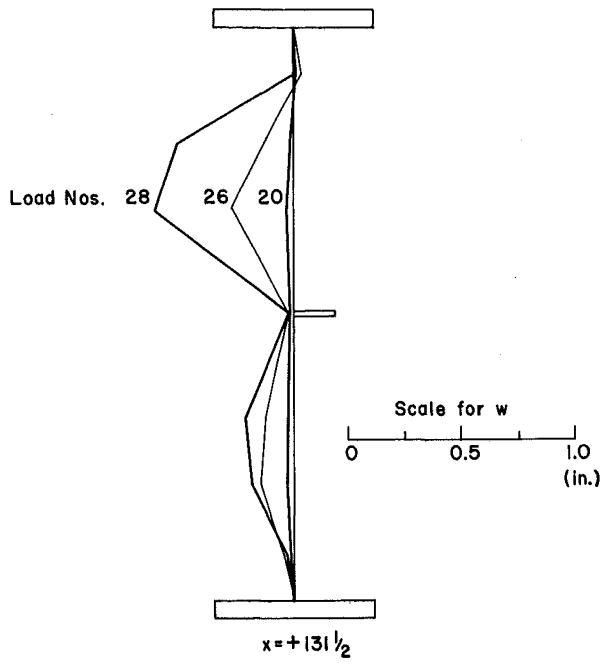

Fig. 32 Web Deflections (Test LS4-T2)

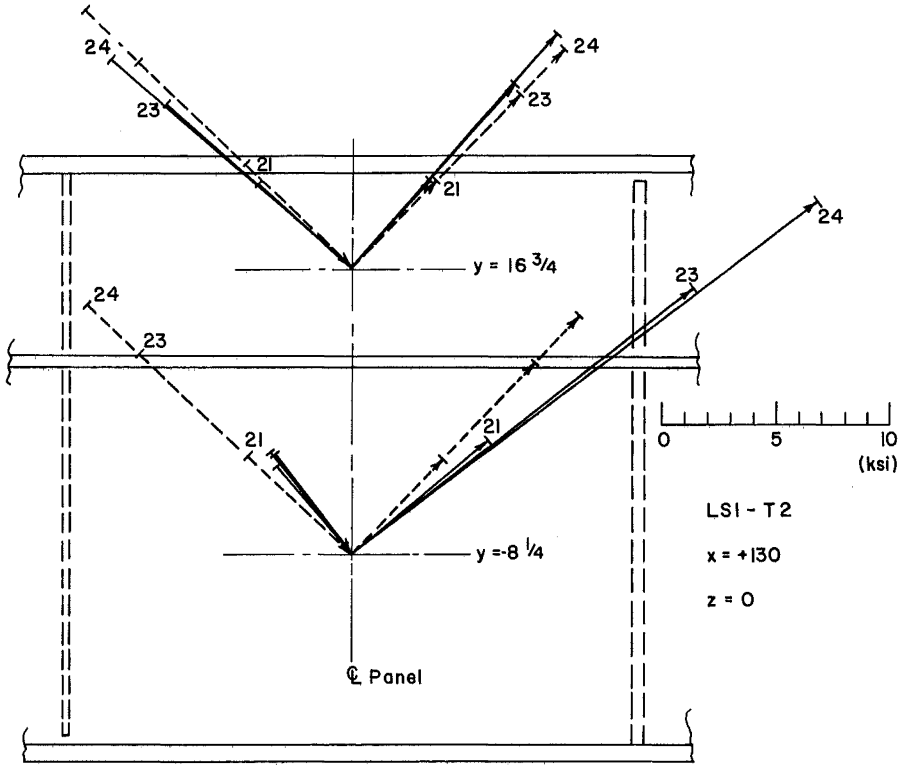

Fig. 33 Principal Stresses in Web of Girder LS1, Test T2

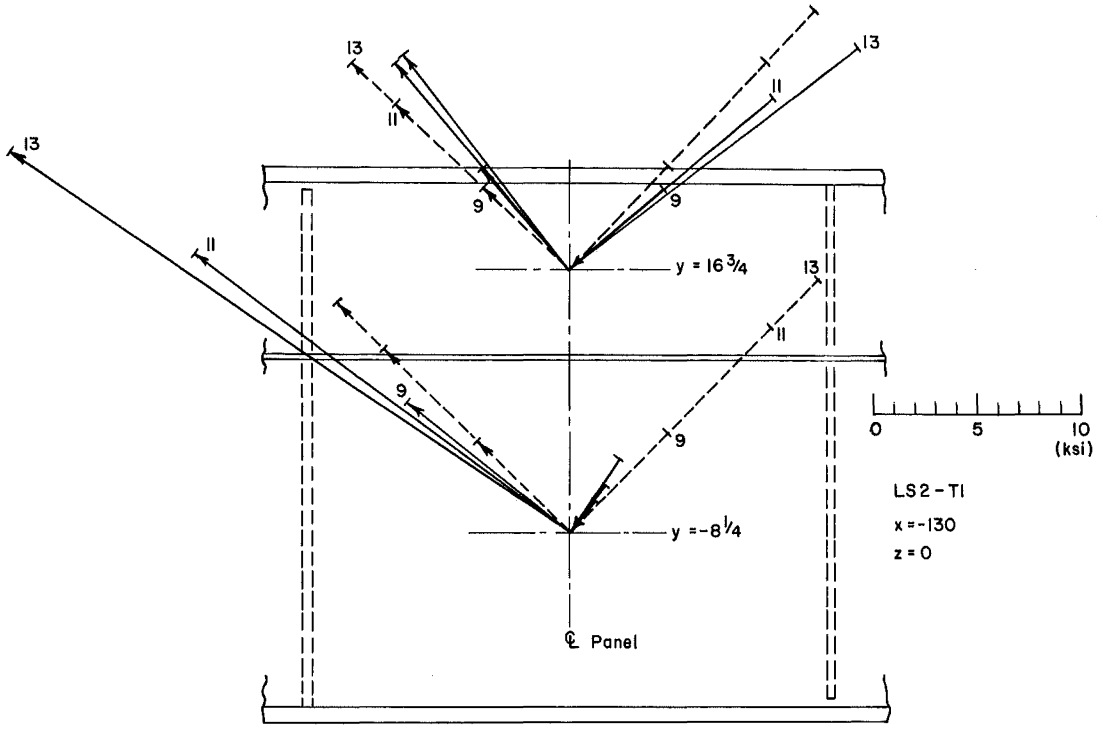

Fig. 34 Principal Stresses in Web of Girder LS2, Test T1

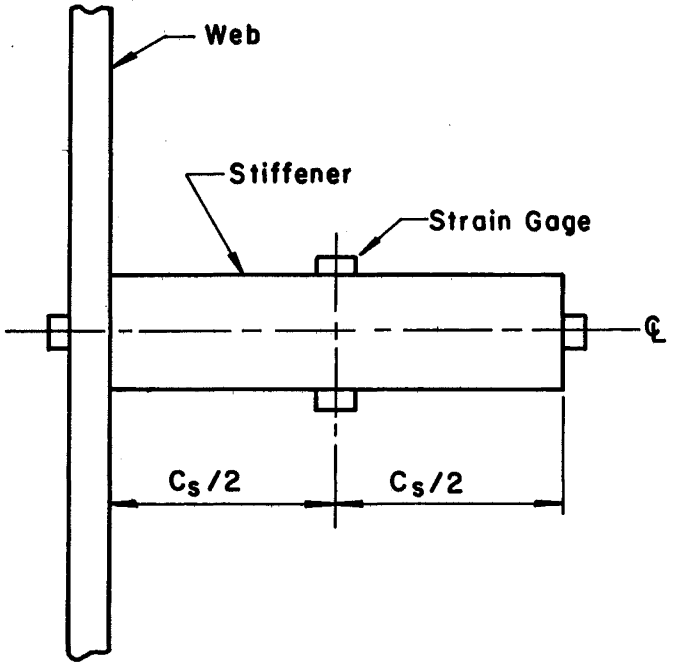

Fig. 35 Locations of Strain Gages on Stiffeners

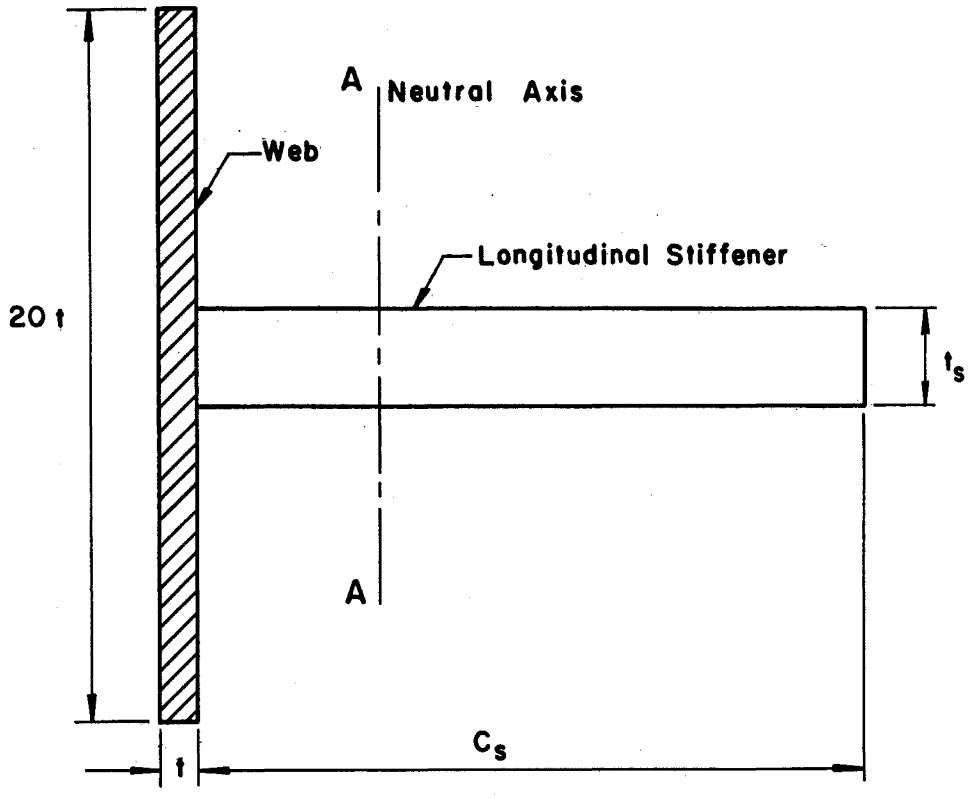

Fig. 36 Assumed Stiffener Section

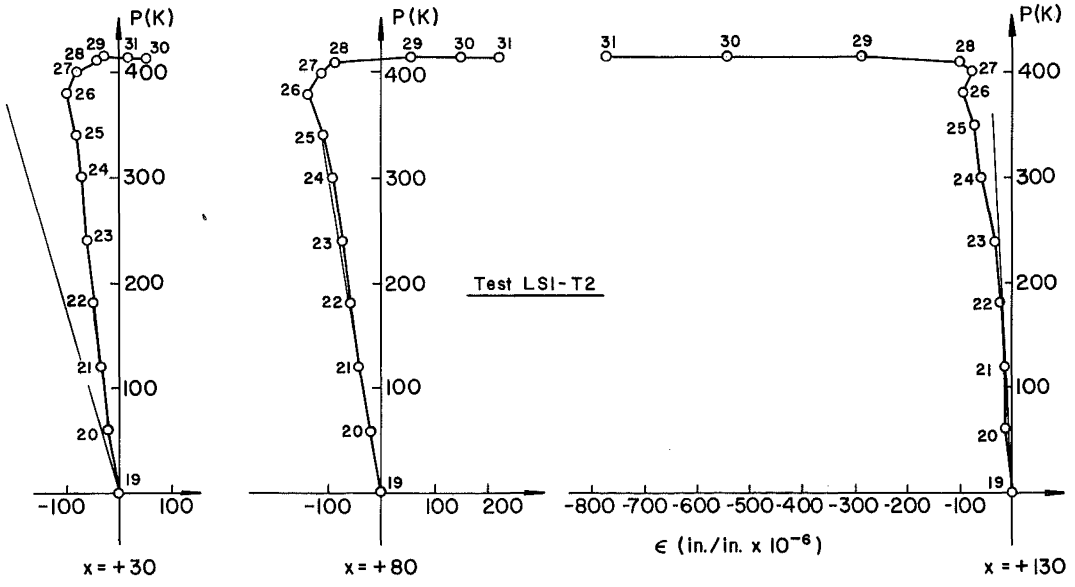

Fig. 37 Longitudinal Stiffener Axial Strains, Test LS1-T2

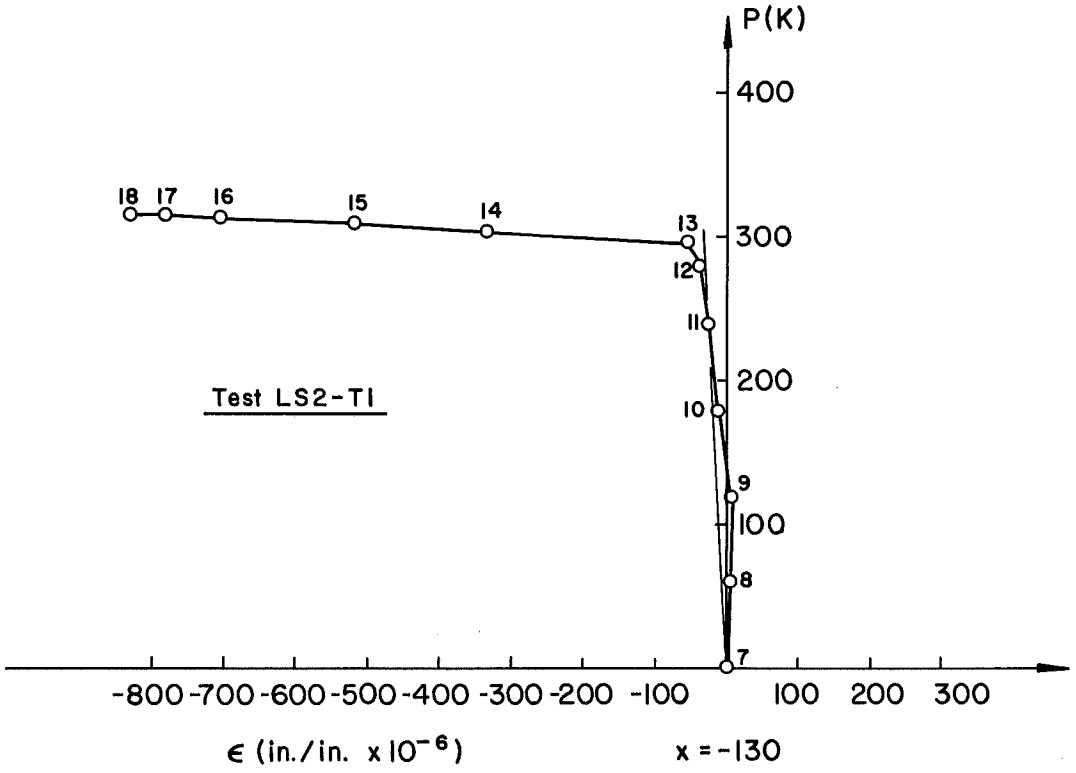

Fig. 38 Longitudinal Stiffener Axial Strains, Test LS2-T1

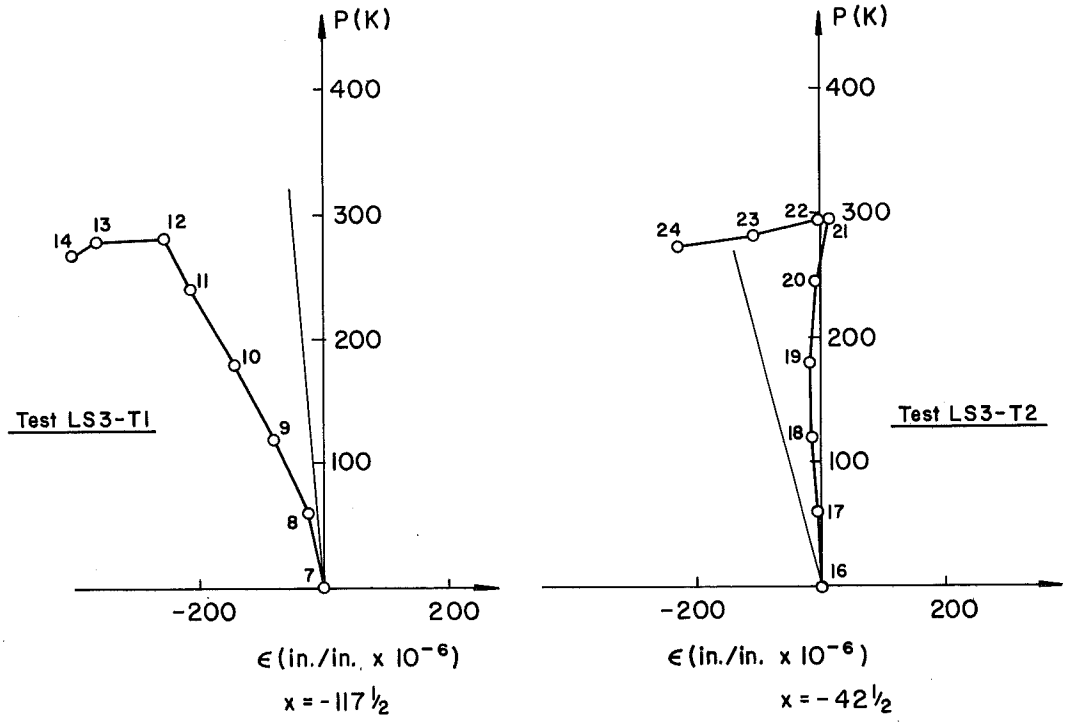

Fig. 39 Longitudinal Stiffener Axial Strains, Tests LS3-T1 & T2

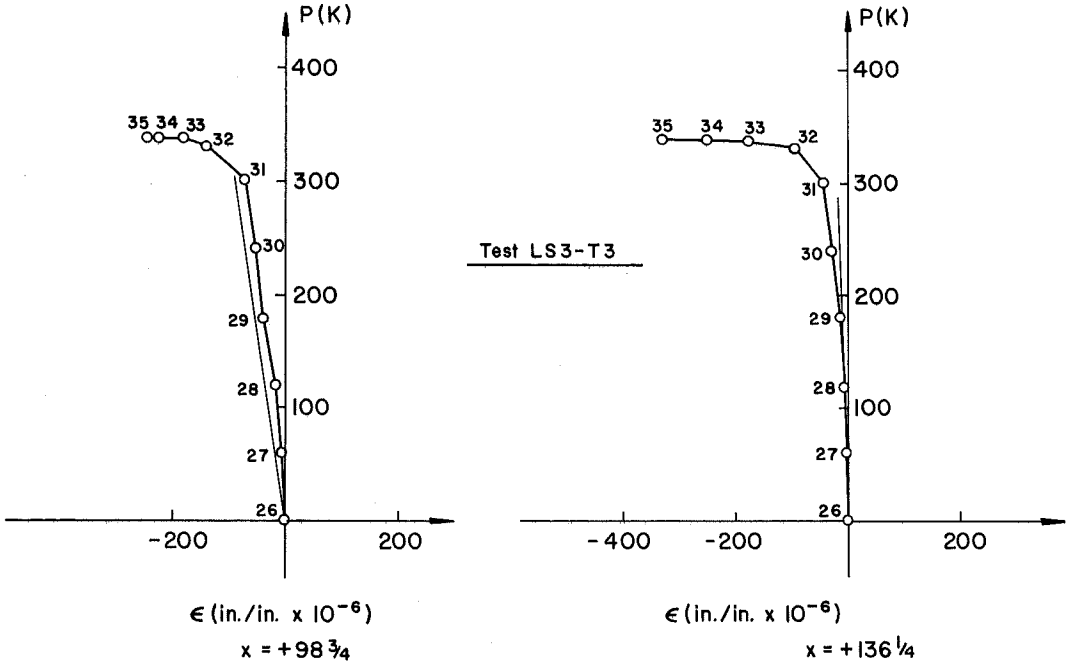

Fig. 40 Longitudinal Stiffener Axial Strains, Test LS3-T3

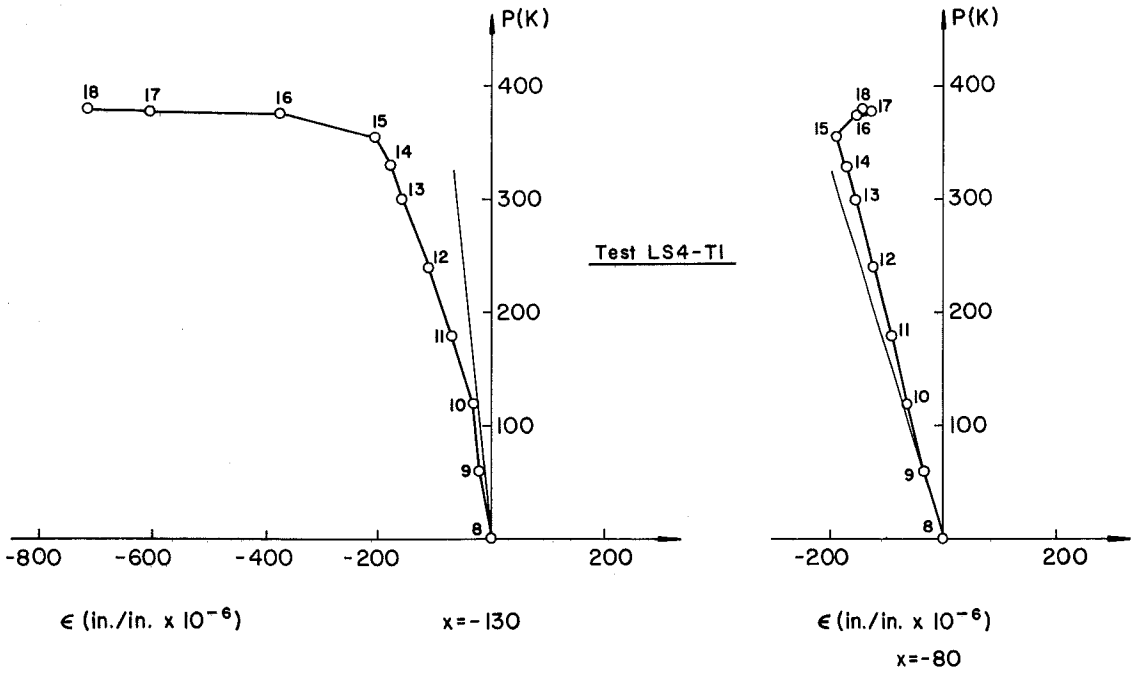

Fig. 41 Longitudinal Stiffener Axial Strains, Test LS4-T1

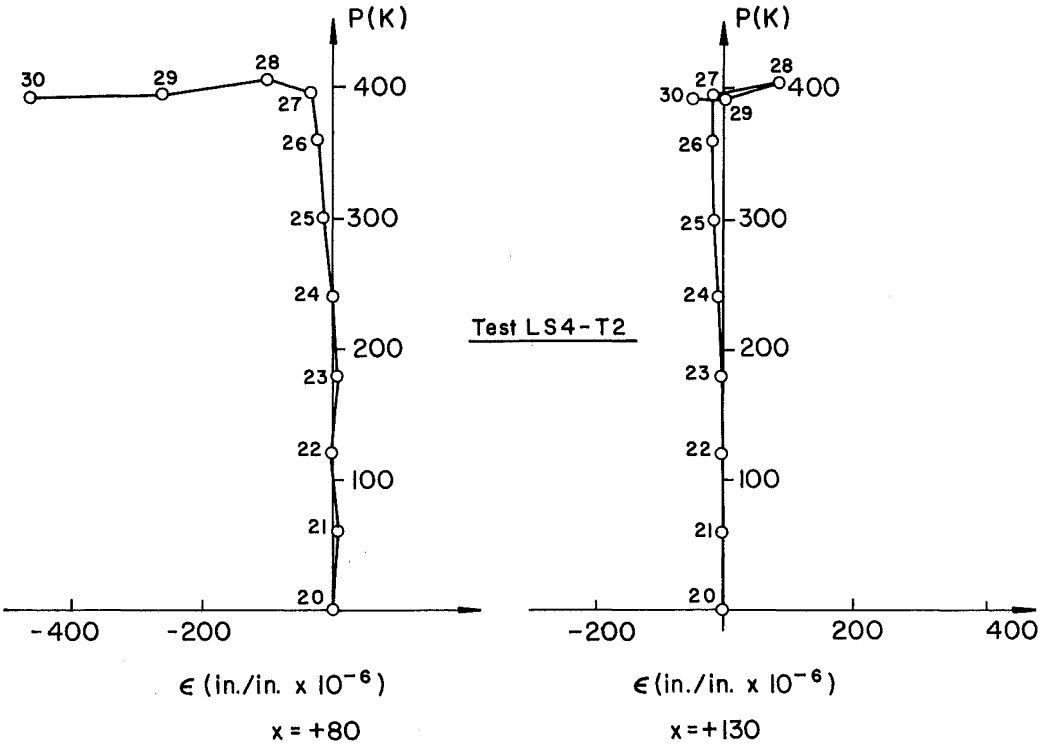

Fig. 42 Longitudinal Stiffener Axial Strains, Test LS4-T2

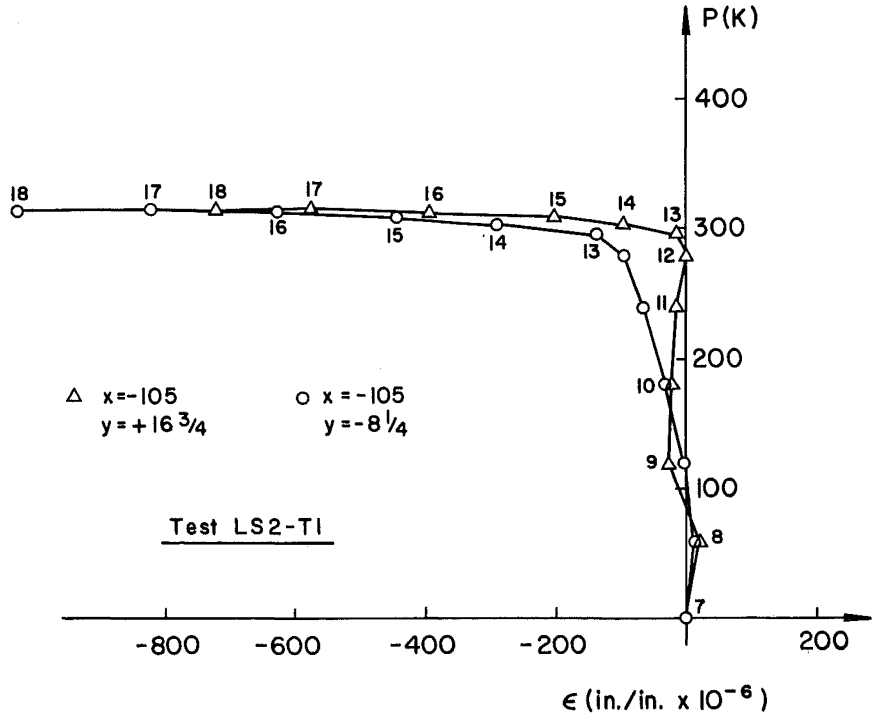

Fig. 43 Transverse Stiffener Axial Strains, Test LS2-T1

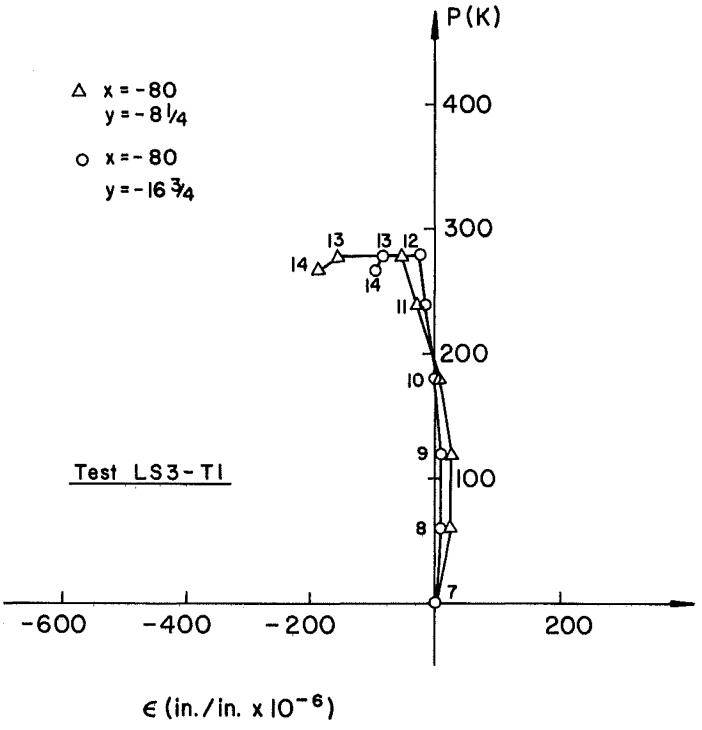

Fig. 44 Transverse Stiffener Axial Strains, Test LS3-T1

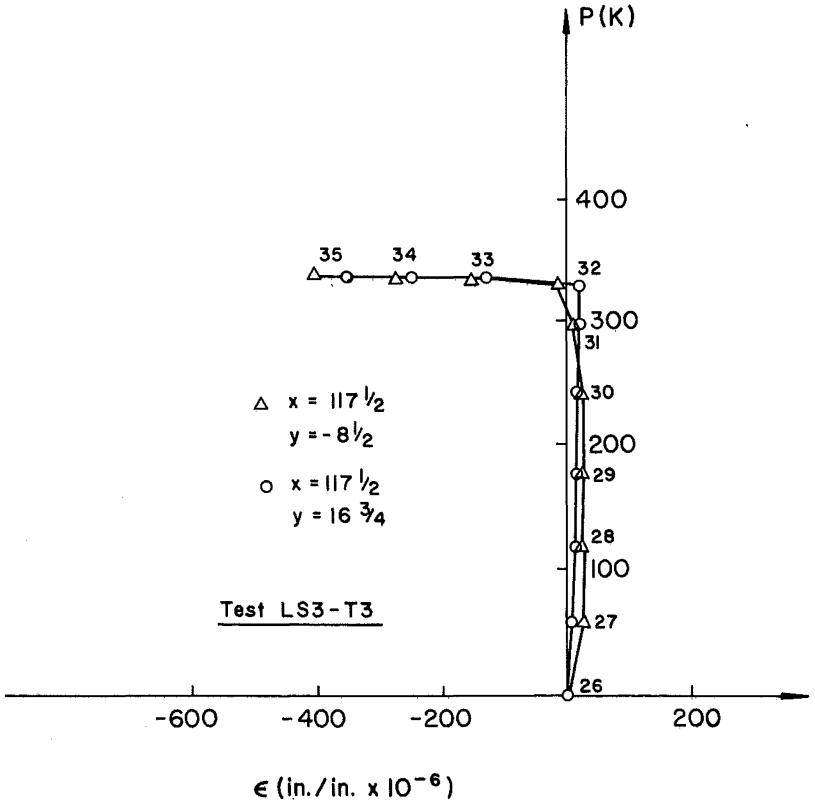

Fig. 45 Transverse Stiffener Axial Strains, Test LS3-T3

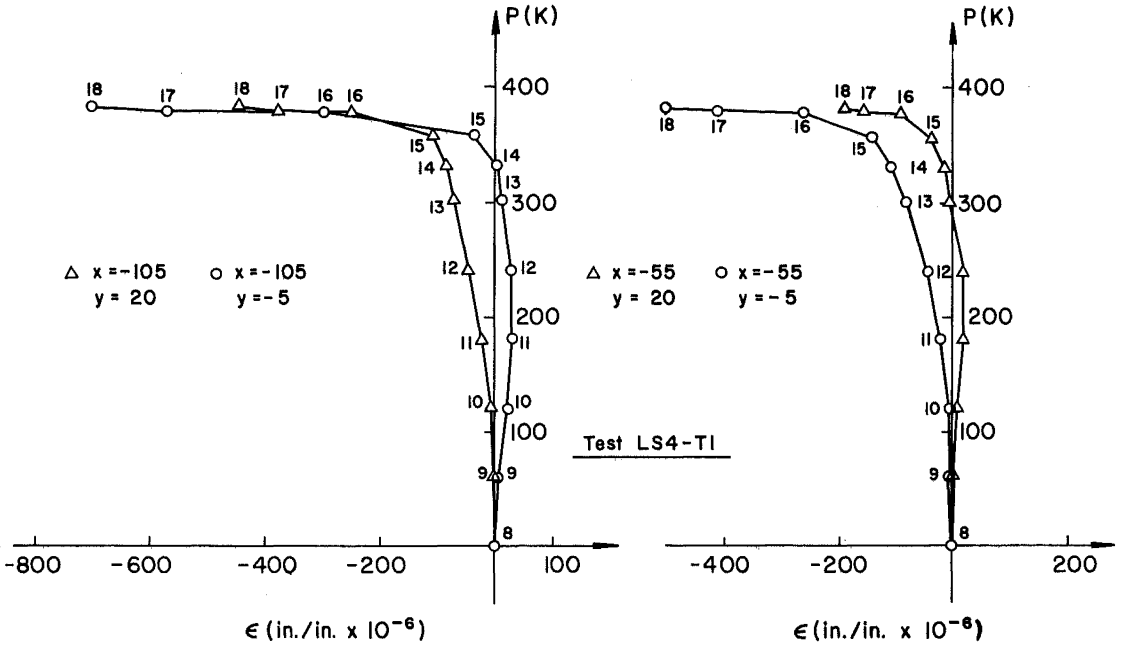

Fig. 46 Transverse Stiffener Axial Strains, Test LS4-T1

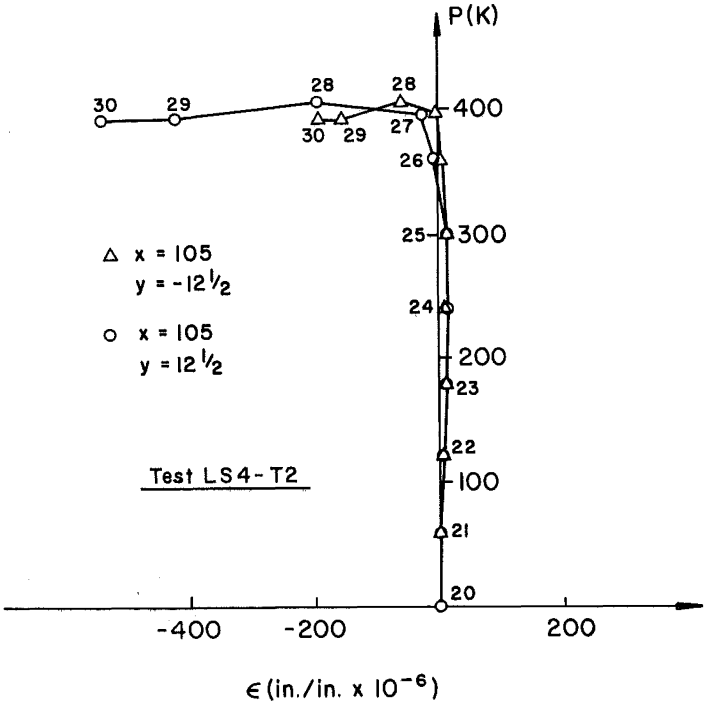

Fig. 47 Transverse Stiffener Axial Strains, Test LS4-T2

8. REFERENCES

1. K. Basler and B. Thürlimann
   STRENGTH OF PLATE GIRDERS IN BENDING, Proc., ASCE, Vol. 87, No. ST6, August, 1961

2. K. Basler
   STRENGTH OF PLATE GIRDERS IN SHEAR, Proc., ASCE, Vol. 87, No. ST7, October, 1961

3. K. Basler
   STRENGTH OF PLATE GIRDERS UNDER COMBINED BENDING AND SHEAR, Proc., ASCE, Vol. 87, No. ST7, October, 1961

4. K. Basler, B. T. Yen, J. A. Mueller and B. Thürlimann
   WEB BUCKLING TESTS ON WELDED PLATE GIRDERS, Bulletin No. 64, Welding Research Council, New York, September, 1960

5. American Institute of Steel Construction, Inc.
   MANUAL OF STEEL CONSTRUCTION, 6th Edition, 1963

6. P. B. Cooper
   BENDING AND SHEAR STRENGTH OF LONGITUDINALLY STIFFENED PLATE GIRDERS, Fritz Engineering Laboratory Report No. 304.6, September, 1965

7. P. B. Cooper
   PLATE GIRDERS, Chapter 8 of "Structural Steel Design", The Ronald Press, 1964

8. Klöppel, K. and Scheer, J. S.
   BEULWERTE AUSGESTEIFTER RECHTECKPLATTEN, Verlog von Wilhelm Ernst & Sohn, Berlin, 1960

9. Massonnet, C.
   STABILITY CONSIDERATIONS IN THE DESIGN OF STEEL PLATE GIRDERS, Proc., ASCE, Vol. 86, No. ST1, January, 1960

9. ACKNOWLEDGMENTS

This report was prepared as part of a research project on longitudinally stiffened plate girders conducted in the Department of Civil Engineering, Fritz Engineering Laboratory, Lehigh University, Bethlehem, Pennsylvania. Professor W. J. Eney is Head of the Department and Laboratory and Dr. L. S. Beedle is Director of the Laboratory.

The sponsors of the research project are the Pennsylvania Department of Highways, the U. S. Department of Commerce-Bureau of Public Roads, the American Iron and Steel Institute, and the Welding Research Council. The research work is supervised by the Lehigh University Welded Plate Girder Subcommittee of the Welding Research Council. The interest and financial support of the sponsors and encouragement of the Committee are gratefully acknowledged.

The authors wish to thank the Project Directors, Dr. Theodore V. Galambos and Dr. Alexis Ostapenko, for their suggestions and guidance in planning and conducting the tests and in preparing the report. Assistance during the testing program was provided by Michael A. D'Apice and Kyle E. Dudley. Miss Marilyn Courtright typed the report, John M. Gera prepared the drawings, and Richard N. Sopko took the photographs of the test specimens.